A Novel Energy Harvesting Aware Routing Protocol for Underwater Wireless Sensor Networks

Sevda Deldouzi

A Thesis in

The Department

of

Electrical and Computer Engineering

Presented in Partial Fulfillment of the

Requirements for the Degree of Master of Science

at Concordia University

Montreal, Quebec, Canada

December 2022

CONCORDIA UNIVERSITY

School of Graduate Studies

This is to certify that the thesis

prepared By: Sevda Deldouzi

Entitled: A Novel Energy Harvesting Aware Routing Protocol for Underwater Wireless Sensor Networks

and submitted in partial fulfillment of the requirements for the degree of

Master of Science (Electrical and Computer Engineering)

complies with the regulations of this University and meets the accepted standards with respect to originality and quality.

Signed by the Final Examining Committee:

_____ Chair
Dr. Amir Aghdam

_____ External Examiner
Dr. Sandra Céspedes

_____ Internal Examiner
Dr. Amir Aghdam

_____ Supervisor
Dr. Rodolfo Coutinho

Approved by _____
Dr. M. Zahangir Kabir, Graduate Program Director

December 13, 2022

_____
Dr. Mourad Debbabi, Dean
Gina Cody School of Engineering and Computer Science

Abstract

A Novel Energy Harvesting Aware Routing Protocol for Underwater Wireless Sensor Networks

Sevda Deldouzi

Underwater wireless sensor networks (UWSNs) have the potential to empower smart ocean applications. However, the widespread use of UWSN applications has been limited due to the many daunting challenges incurred for underwater wireless acoustic communication. Moreover, underwater wireless communication is energy-hungry, which confines UWSN deployment to small-scale due to the risks and costs of missions for at sea replacement of the nodes' battery. The energy harvesting capability of underwater sensor nodes is an important characteristic that has been overlooked in the literature. In this thesis, we study the data routing process in UWSNs with energy harvesting capabilities. We proposed a novel opportunistic routing protocol, named RELOR, that is the first in the literature to consider the energy harvesting capability of underwater sensor nodes during routing decisions. RELOR implements a learning framework for the best selection of the forwarder nodes based on the observed environment conditions. We conduct extensive simulations to compare the performance of the proposed protocol to the state-of-the-art solution. Obtained results show that RELOR outperforms the related work in terms of packet delivery ratio, end-to-end latency, and nodes' energy consumption.

Acknowledgements

I would like to express my deepest gratitude to my supervisor, Professor Coutinho. Without his assistance and dedicated involvement in every step of the process, this thesis would never have been accomplished. I would like to thank you very much for your support and understanding over the past two years.

Also, special thanks to my lifemate, Kasra, for his endless love and encouragement throughout my master's journey. My appreciation for your support goes beyond what you can imagine. Thank you for providing me with a safe and peaceful space to concentrate on my work. I love you!

I want to thank my sister by heart, Sarvin, for supporting me through my hardest days and encouraging me to not give up on my dreams. Thank you for being such a wonderful friend.

And last but not least, I would like to thank my beloved parents. I will always be grateful to them. Their encouragement and belief in me have kept me motivated and inspired. Without them I wouldn't have been able to accomplish my goals. My dad for his unwavering support and insights and my mom for her never-ending love and care throughout my entire life. Thank you for being there for me whenever I needed you and giving me this much love and support even with this long distance between us. I cannot express my gratitude enough for you. I love you so much!

Contents

List of Figures

List of Tables

List of Abbreviations

ACK	Acknowledge
ASV	Autonomous Surface Vehicle
AUV	Autonomous Underwater Vehicle
DBR	Depth-Based Routing
FBR	Focused Beam Routing
IoUT	Internet of Underwater Things
MDP	Markov Decision Process
MFC	Microbial Fuel Cell
OR	Opportunistic Routing
PDR	Packet Delivery Rate
PMS	Power Management System
RF	Radio Frequency
RL	Reinforcement Learning
TENG	Triboelectric Nanogenerators
UWSN	Underwater Wireless Sensor Network
VBF	Vector-Based Forwarding

Chapter 1

Introduction

1.1 Underwater Wireless Sensor Networks

Oceans account for approximately 96% of the world's water resources. The vast areas of the ocean haven't been explored due to a variety of restrictions, including inaccessibility of the underwater environment, high costs of ship missions, etc. Underwater sensor networks (UWSNs) have great potential to help change the aforementioned reality. UWSN was proposed as an alternative to traditional wired and communicationless methods for observing and exploring aquatic environments [1]. Typically, UWSNs will be composed of heterogeneous surface and underwater nodes equipped with different sensing instruments and different communication technologies (e.g., acoustic, optical, magneto-inductive modems) [2]. In this special kind of ad hoc network, underwater and surface nodes will wirelessly communicate with each other and collaborate to monitor underwater variables of interest and report gathered data from the underwater environment to monitoring centers [3].

As mentioned earlier, several communication mediums are available, each with its own advantages and disadvantages that must be considered before selecting one.

- **Radio Frequency** UWSNs can be equipped with radio frequency electromagnetic waves in order to achieve high data rates over a short range of communication [4]. Electromagnetic communication produces different data rates in

freshwater and seawater. Due to water's high permittivity and electrical conductivity, radio waves propagate differently from atmospheric waves [5]. Due to the high attenuation of radio frequencies, they are not suitable for long-range underwater communication [6]. Radio-frequency communications are, however, used in a variety of short-range navigation, sensing, and communication applications [7].

- **Optical** When compared to other approaches to underwater communication, optical USWN communication offers the highest data rates (up to Gbps), as well as the lowest delays [4]. In addition, due to its high propagation speed (i.e., the speed of light), it can be applied to real-time underwater tasks [7]. Due to the unique characteristics and environment of the underwater environment, underwater optical communication is subject to absorption and scattering problems, which can reduce the quality of data transmission over long distances [4]. Furthermore, transmitting optical signals requires the narrow laser beams to be aimed with a high degree of precision, which is difficult in an underwater environment with mobile sensors [8].

- **Acoustic** Underwater acoustic communication is the most commonly used method for implementing underwater sensor networks. Acoustic communication offers the advantage of achieving long communication ranges of up to 20 kilometers [9]. Low sound speed, an increasing attenuation with frequency, and multipath propagation are the main characteristics of underwater acoustic communication [10]. There is a limit to the amount of bandwidth available (5 kHz) due to the better performance of acoustic propagation at low frequencies (10–15 kHz) [7]. There are several challenges associated with high-speed acoustic communication in UWSNs, such as limited bandwidth, high transmission losses, multipath fading, and Doppler effect [11].

As part of an UWSN, routing protocols are necessary to establish communication and enable fdata transmission between the sensor nodes and the base stations.

Great deal of attention has been received on the different types of underwater routing protocols [12]–[19]. In recent years, opportunistic routing (OR) protocols have been proposed to increase the performance of the network [1], [12], [16], [20], [21]. Opportunistic routing (OR) is a promising paradigm that takes advantage of the broadcast nature of the wireless medium and selects the potential group of nodes (candidates) to forward the data [22].

1.1.1 Applications

Underwater sensor networks have the potential to be used in a wide variety of offshore and deep ocean applications, which can be divided into 5 categories [23]:

1. **Environmental Monitoring** Nodes of underwater sensors may be deployed in an area of interest for the purpose of collecting and reporting data regarding variables of interest, such as temperature, salinity, and pH. Parameters such as these can be used to monitor the ocean's aquatic environment in various ways, such as water quality monitoring [24], chemical or biological pollution monitoring [25], oil and gas pipeline monitoring [26], pressure and temperature monitoring [27].

2. **Underwater Exploration** Sensor nodes can be used to monitor the underwater environment, its characteristics, properties, or any object of interest for a variety of purposes, including monitoring marine life and locating natural resources. For instance, Coutinho et al. [28] used UWSNs to monitor North Atlantic Right Whales and gather data necessary to protect NARW populations from extinction. The authors of [29] have proposed a UWSN for the discovery and excavation of mineral resources underwater.

3. **Disaster Prevention** Disaster prevention applications are among the most critical applications of IoUT. In general, water-based natural disasters are more dangerous and result in enormous destruction to the planet. In order to prevent such disasters, IoUT is widely used to detect floods [30], earthquakes [31],

and tsunamis [32], and underwater volcanic eruptions, and to offer early warning services.

4. **Military** Military applications can also be achieved with UWSNs. Cameras, imaging sonars, and metal detectors are among the sensors used for detecting underwater mines [33], locating submarines [34], as well as monitoring and surveillance systems [35].

5. **Others** There are several other applications for UWSNs, such as sports, navigation, and localization. The authors of [36] proposed a system that would monitor swimmer performance and transmit the information to the couch or to other swimmers. Authors in [37] have developed an anchor-free localization algorithm that relies on information about adjacent nodes for underwater sensor location assistance.

1.1.2 Architecture

Underwater wireless sensor networks consist of underwater sensor nodes, surface sonobuoys (sinks) and autonomous underwater vehicles [8]. Typically, underwater sensor nodes are the main components of the network. The sensors monitor and collect data (such as pressure, temperature, biological or chemical elements, etc.) from areas of interest and transmit it to sinks on the surface through acoustic communication. The sensor nodes may be stationary, fixed, either anchored to surface buoys or the seafloor, or mobile, floating at different depths. The sink nodes are responsible for establishing communication between underwater nodes and onshore stations. As data arrive at sinks (through acoustic channels), the sinks transmit the information to the remote monitoring center (through radio channels). The sinks are equipped with both acoustic and RF modems, and they may be buoys, ships, or ASVs. Additionally, AUVs (Autonomous Underwater Vehicles) can also be included as an optional component of the UWSN. These devices can be used to collect and forward data or to extend the range of communication. In terms of architecture,

UWSNs can be either two-dimensional or three-dimensional. In 2D networks, sensor nodes are anchored to the bottom of the ocean by anchors. On the other hand, in 3D UWSNs, the sensor nodes float at various depths in the ocean. Sensors can either be mobile or non-mobile. Fig. 1.1 represents the network architecture for UWSNs with non-mobile nodes anchored to the ocean floor in various depths, AUVs, multiple sinks and on-shore monitoring center.

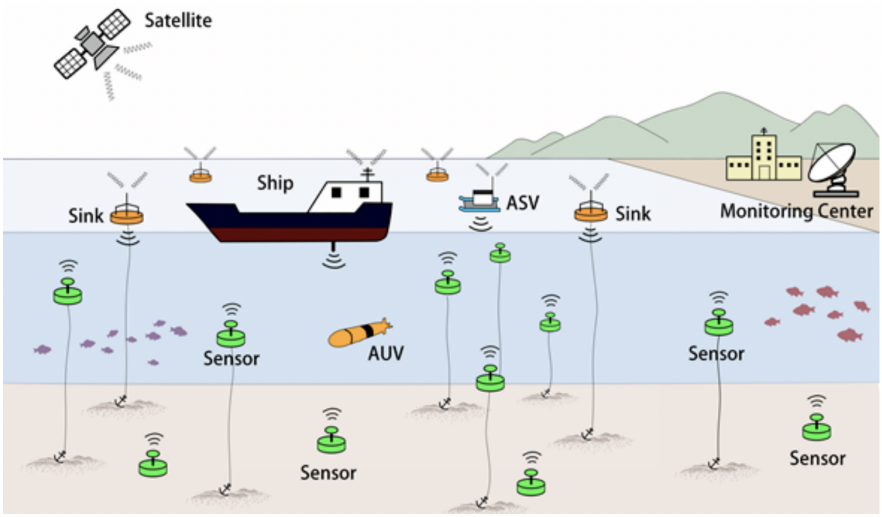

FIGURE 1.1: Network architecture of UWSNs [23]

1.1.3 Challenges

To date, significant progress has been made in sensing and communication technologies for UWSNs. However, many are fundamental challenges that require further investigation. Due to the harsh underwater environment and the properties of acoustic communication, the underwater acoustic sensor network faces several challenges. The challenges include:

- **Path Loss** During the propagation of sound from the underwater environment, some of its strength converts into heat. There are two main categories in which energy loss occurs during sound wave propagation [38].
  - Geometric Spreading Loss: It represents the power loss incurred during the propagation process between the source and the destination nodes.

As the acoustic wavefront spreads, it occupies an increasing area, and therefore, its magnitude diminishes. There are two methods for modeling spreading power loss, including spherical spreading and cylinder spreading, depending on the source and working environment [39].

- Attenuation: During the propagation of the acoustic signal, the energy is converted into heat and absorbed by the underwater environment. The attenuation loss is directly proportional to the frequency and distance [40].

- **Noise** Underwater acoustic channels are subject to a variety of noises, including:

  - Ambient Noise: The ambient noise in the ocean can be divided into four major categories: turbulence, shipping, wind, and thermal noise. As a result of waves or tides, turbulent noise is generated by surface disturbances which generate low frequencies. Due to the large number of ships in the ocean, acoustic communication is subject to high traffic shipping noise. A wind noise occurs when a wave breaks or when bubbles are created by the air [40].

  - Man made Noise: As a result of heavy machinery usage (pump, power plant, fishing, military, etc.) these noises are produced.

- **Multipath** A multipath effect occurs when a wave is transmitted from the source node to the destination node via two or more paths. At the destination node, the two arriving signals may interfere with one another. It is particularly important to note that in the shallow underwater environment, the factors such as the acoustic speed, the temperature, the salinity, etc. will differ according to the depth of the water. Therefore, shallow water environments can be divided into several layers from the surface to the bottom. It is possible for an acoustic wave to be transmitted and reflected within many layers, and

multiple arrivals of the same signal may be detected at the receiver, resulting in a multipath effect [39].

- **Energy Constraints** One of the daunting challenges that limit large-scale deployments of UWSNs is the high energy cost involved in the UWSN operation. Underwater sensor nodes are powered by batteries, which limits the lifetime of underwater monitoring missions. Besides, underwater acoustic communication is energy-hungry. The energy cost for data transmission is of the order of dozen of Watts [41]. This highly impacts the content delivery since designed routing protocols often overuse a set of nodes selected as relays for multi-path data delivery. The overuse of such nodes will lead to depleting their energy quickly, which will result in network partitions and disconnections since UWSN often relies on low-density deployments. Hence, periodic ship missions for underwater sensor nodes immanence and battery replacements would be required. However, such missions are costly from time and monetary points of view, subject to weather conditions, and pose many dangers to human lives.

- **Dynamic Network Topology** controlled and uncontrolled underwater nodes' mobility will affect the network topology and impact sensing and communication tasks and the movements are decreasing the performance of routing protocols [42].

Other challenges in this area include high and variable delay, low bandwidth, shadow zones, and temporary loss of connectivity [8], [10].

1.2 Thesis Statement and Contribution

This thesis presents the design of the first opportunistic routing protocol for underwater sensor networks that can harvest energy from the environment. We propose and design the REinforcement Learning-based energy harvesting-aware Opportunistic Routing (RELOR) protocol for underwater sensor networks. The RELOR protocol considers the energy cost and harvestable energy of next-hop nodes when selecting the next-hop forwarder nodes at each hop. The main goal is to select energy-efficient opportunistic routing paths from source nodes to the surface sonobuoy aimed at improving data delivery reliability while prolonging the network lifetime. To the best of our knowledge, RELOR protocol is the first opportunistic routing protocol that takes advantage of energy harvesting mechanisms when deciding suitable next-hop forwarder nodes for multi-hop data routing in UWSNs. In order to accomplish this, the next-hop forwarders set selection problem is modeled as a Markovian decision problem (MDP). A reward function that considers link reliability, expected energy cost, and harvestable energy information was devised, aimed at driving optimized decisions regarding next-hop forwarder selections. Some challenges that are mentioned in section 1.1.3 such as energy limitations are addressed with our protocol. And finally, an extensive performance evaluation was conducted to assess the performance of the RELOR protocol in comparison to the HyDRO [43] and CARMA [44] routing protocols. The DESERT underwater simulator [45], [46] was used to evaluate the performance of the proposed protocol under realistic UWSN deployments and environmental conditions. The results and performance evaluation of our work have been published in the International Conference on Modeling, Analysis and Simulation of Wireless and Mobile Systems (ACM MSWiM) [47].

1.3 Thesis Outline

The remainder of this thesis is organized as follows. Chapter 2 provides an overview of energy harvesting methods for underwater wireless sensor networks. Chapter 3 surveys the literature about routing protocols in UWSNs. Chapter 4 proposes a reinforcement learning-based harvesting-aware routing protocol for rechargeable underwater sensor networks. Chapter 5 presents performance evaluation and provides comparison between the proposed work and other protocols. Finally, Chapter 6 summarizes the contributions of this thesis and we present some research directions for future works.

Chapter 2

Energy Harvesting in Underwater Wireless Sensor Networks

2.1 Introduction

Energy harvesting methods provide the necessary mechanism for converting ambient energy, from a variety of sources, into electrical energy. The general idea is to scavenge ambient energy and transform it into useful electrical energy. Energy harvesting has been extensively considered to recharge batteries of sensor nodes in terrestrial wireless sensor networks [48]–[55]. In recent years, energy harvesting has also been considered in the design of networking protocols and task offloading mechanisms in IoT applications [56]–[59]. However, energy harvesting is overlooked when it comes to Internet of Underwater Things (IoUT) devices. In this Chapter, we discuss the mechanism that makes it possible to harvest energy in IoUT applications. In Section 2.2, six different types of energy harvesting are described and their related work is discussed.

2.2 Energy Harvesting in Underwater Wireless Sensor networks

UWSNs may benefit from energy harvesting by recharging the batteries of sensor nodes and extending the network's lifetime. Current approaches for energy harvesting underwater wireless sensor networks (EH-UWSNs) can be classified into six categories, based on the source and mechanism used to harvest energy from the environment, as: kinetic, microbial fuel cells, solar energy, seawater batteries, galvanic energy, and ultrasonic waves. By doing so, we discuss the working principle, advantages, and challenges of each approach. Besides, we highlight works in the literature that design and implement the considered energy harvesting mechanisms. Table 2.1 provides a summary of each research study in EH-UWSNs.

TABLE 2.1: Summary of Energy Harvesting Methods

Literature	**Category**	**Harvesting Capability**	**Advantages**	**Disadvantages**	**Method**
Diab et al. (2019) [60]	Kinetic	175 μW	Wide frequency range, low directivity, minimum sensor geometric dimensions	Dependency of harvesting power to the sensor-transmitter distance	Piezoelectric
Kim et al. (2020) [61]	Kinetic	17 mW	Higher output using a frequency tuning method	Lower water flow speed compared to actual deep ocean flow	Piezoelectric
Toma et al. (2015) [62]	Kinetic	350 μW/cm^3	Low dependency on resonant frequency of the piezoelectric element	Incompatible size for sensor nodes	Piezoelectric
Cha et al. (2013) [63]	Kinetic	2 μW	Thorough mathematical model to compare with experiments	Only tested in laboratory environment	Piezoelectric
Qureshi et al. (2017) [64]	Kinetic	820 μW	High outputs compared to other works	Scalability, no laboratory experiments	Piezoelectric

Table 2.1 – *Continued from previous page*

Literature	**Category**	**Harvesting Capability**	**Advantages**	**Disadvantages**	**Method**
Wang et al. (2015) [65]	Kinetic	10 mW	Lightweight , low cost	Floated on the water (not suitable for deep applications)	TENG (Triboelectric Nanogenerators)
Zhang et al. (2022) [66]	Kinetic	95.5 μW/m	Cost-effective	Low output in deep ocean	TENG
Donovan et al. (2011) [67]	MFC (Microbial Fuel Cells)	2.5 W in short bursts. (3.4 mW continuous average power)	Converting low output of SMFC (Sediment Microbial Fuel Cells) to several watts	High implementation costs	SMFC
Huang et al. (2013) [68]	MFC	153 mW/m^2	Relatively high output	Not tested in real environment	SMFC
Umaz et al. (2020) [69]	MFC	10.89 μW – 108.9 mW	Low charging time, dynamic load ranges	Not tested in real environment	Power Management System (PMS) for MFC

Table 2.1 – *Continued from previous page*

Literature	**Category**	**Harvesting Capability**	**Advantages**	**Disadvantages**	**Method**
Carreon-Bautista (2015) [70]	MFC	7.8 μW (MFC load: 8 kΩ) 1.6 mW(MFC load:100Ω)	Dynamical adaptation to achieve MPP, adjusting the converter's power consumption for maximum efficiency	Not tested in real environment	Converter for MFC
Zhang et al. (2012) [71]	MFC	95 mW	Providing thorough comparison between two different PMS types	Only provide analytical results	Converter for MFC
Meehan et al. (2010) [72]	MFC	95 mW	Harvesting larger energy for a longer time period compared to previous works	Relatively long charging time (9.3 h), bigger surface	PMS for MFC
Zayan et al. (2018) [73]	Solar Energy	3.29 W/m^2 (in 5 meter depth)	Better performance in deeper environments rather than Tl-based solar cells	Low outputs in the deep ocean	InGaP Solar cells

Table 2.1 – *Continued from previous page*

Literature	**Category**	**Harvesting Capability**	**Advantages**	**Disadvantages**	**Method**
Amurta et al. (2013) [74]	Solar Energy	1.5 W	Saving energy for nights	Low outputs in the deep ocean, Not tested in real environment	Solar cells
Kamal et al. (2019) [75]	Solar Energy	2.2 and 4 V for monoly-ocrystalline and poly-ocrystalline	Comparing two different kinds of cells and finding optimum depth according to light attenuation and cooling effect	Not tested in the ocean environment	Mono and Polycrys-talline solar cells
Jenkins et al. (2013) [76]	Solar Energy	0.7 mW/cm^2 at 9.1 meters	Better performance compared to silicon cells	Performance drop by 10 % in depths more than 2 m	InGaP solar cells
Abdellatif et al. (2020) [77]	Solar Energy	4.2 V at 3 meters	Small dimension	Not suitable for deep ocean	Mono-crystalline solar cells
Kim et al. (2014) [78]	Seawater battery	5 and 24 V	Relatively high output	Big dimensions	Seawater batteries
Shinohara et al. (2009) [79]	Seawater battery	13 W in average	Relatively high and stable output	Big dimensions	Seawater batteries

Table 2.1 – *Continued from previous page*

Literature	Category	Harvesting Capability	Advantages	Disadvantages	Method
Rezaei et al. (2012) [80]	Galvanic Energy	768 mW	Suitable for low power sensor nodes, Operating for a longer time	Low output	Galvanic cells
Sivakami et al. (2019) [81]	Galvanic Energy	1.1 V	Testing different materials for anode and cathode to reach maximum output	Big dimensions	Galvanic cells

2.2.1 Water Kinetic Energy Harvesting

In IoUTs, water kinetic energy is harvested from ocean currents or tides in order to recharge the batteries of underwater sensor nodes. The use of motion for energy harvesting makes kinetic energy less dependent on weather conditions, seasonality, temperature or daylight than wind or solar energy harvesting. The most common means of harvesting water kinetic energy is through the use of rotors, piezoelectric materials, and triboelectric nanogenerators (TENGs). The characteristics, working principles, advantages and disadvantages of each one of these common approaches are discussed in the following.

The piezoelectric effect occurs when specific types of materials (e.g., quartz, topaz, etc.) emit an electric charge in proportion to the amount of mechanical stress they are subjected to. Piezoelectric materials are used in underwater applications to harvest energy from vibrations in the water in order to power batteries [82].

A piezoelectric device is used by Diab et al. [60] for harvesting energy from vibrational energy, while an additional low power management circuit is proposed to ensure the optimal power transfer. The performance of this device is dependent to

the transmitter/sensor distance and the incident acoustical field excitation voltage. Maximum output power of 175 µW is harvested with an excitation voltage of 8 Vpp at 5 cm distance from the emitter. Their proposed method has a large frequency range but the harvested energy is dependant to the sensor-transmitter distance. The size of the harvesting device is relatively small (a spherical with radius of 20mm) and it can be implemented with low costs.

Authors in [61] describe a propeller-based underwater piezoelectric energy harvester with a propeller, hitting sticks, and a piezoelectric module. Using an acrylic plate, they can adjust the bending length of a piezoelectric module, resulting in frequency matching and maximum output power of 17 mW at a resistance of 10.8 kΩand a bending length of 80 mm. Frequency tuning allows them to achieve higher outputs. In terms of size, their proposed device is relatively compact (95mm × 35mm × 0.8mm) as well as being cost-effective.

A prototype consisting of a Bristol pendulum and piezoelectric bimorphs was proposed by Toma et al. [62]. Their proposed energy harvester can produce an output of 0.3 mJ to a maximum of 0.6 mJ, with medium wave height of 30 cm and wave period between 3 to 10 seconds (maximum power density of 350 $\mu W/cm^3$) . The energy harvester has low dependency on resonant frequency of the piezoelectric element. Due to the size of the prototype, it cannot be used with underwater sensor nodes (cylinder with the diameter of 26cm and 50cm length). Furthermore, it has a high implementation cost when compared to other works.

Cha et al. [63] presented an energy harvesting method based on base excitation of a piezoelectric composite beam. The energy harvester part consists of a thin aluminum beam sandwiched between two macro-fiber composites. This experiment was conducted in a laboratory environment, in a test tank filled with room temperature tap water. Results of the experiment indicated that the device's output power was approximately 2mW at a nominal base excitation amplitude of 0.37mm and less than 1mW at a nominal base excitation amplitude of 0.73mm.

The authors of [64] designed a piezoelectric (PZT) bimorph energy harvester for

the purpose of harvesting power for pipelines. Using analytic models of pipelines and the amount of energy required, they calculated the dimension of PZT. An output power of 820 μW can be generated by their model with a cantilever of 15 mm length. In order to achieve the desired output power, 15 PZT cantilevers are connected in parallel to produce 12.3 mW.

Triboelectric nanogenerators (TENG) were first proposed in [83]. The TENG harvests energy by coupling contact electrification and electrostatic induction, resulting in high efficiency in the conversion of mechanical energy into electrical energy. A TENG is currently emerging as a lightweight and low-cost method of harvesting energy that will contribute to the development of health care devices, wearable electronics, sensor networks, and the Internet of things, for example. There are several advantages to using them, including their simple structure, environmental friendliness, low manufacturing costs, and high level of safety. Also, these materials are resistant to water due to the fact that their macroscopic, one-dimensional structure prevents humid from contacting their internal structures.

The authors of [65] reported that a rolling-structured, freestanding triboelectric-layer-based nanogenerator (RF-TENG) can be used to harvest energy from low-frequency wave movements. In their proposed design, a peak current of 1 μA and instantaneous output power of up to 10 mW can be achieved over a wide load range, ranging from a short-circuit condition to 10 GΩ. This RF-TENG has the advantage of being lightweight and inexpensive. Considering that this device is designed to float on the surface of the water, it may not be suitable for applications in deep water.

Zhang et al. [66] proposed a network based on Cable structured-TENGs for underwater detection and real-time monitoring. As part of their study they designed and tested the CS-TENG energy harvester. The device was tested in a water tank at a depth of 10 cm and using a wave generator to simulate ocean currents. For a 5 cm-long cable, the maximum peak power density was approximately 95.5 μW/m. As the depth increases, the output will decrease. The energy harvester has a diameter of 2.75 cm, making it relatively small in size. Due to the low cost of the materials

used to manufacture the CS-TENG, it is more cost-effective than other methods.

2.2.2 Microbial Fuel Cells

Microbial Fuel Cells (MFCs) are also a potential source of energy in underwater environments. MFCs generate electricity directly from biodegradable substrates using the metabolic activities of bacteria [68]. Sediment microbial fuel cells (SMFCs) consist of an anode and a cathode. Typically, the anode is buried under sediment, in the absence of oxygen, and the cathode is located above the sediment in water [67]. During the movement of electrons, produced by microorganisms in the sediment, electricity is generated and is stored in a circuit connected to a cell. The most significant disadvantage of MFCs is their low output energy to power UWSN, so power management systems (PMSs) are designed to overcome this problem.

Donovan et al. [67] proposed a power management system that converts low-level power from SMFCs into 2.5 W power. The anode of the SMFC was buried beneath sediment, in an oxygen-free environment, and the cathode was located above it. During each charging cycle, they were able to achieve an output power of 2.5 W in five seconds, whereas the SMCD itself is capable of continuously generating an average power of 3.4 mW. This PMS has relatively high implementation costs.

Huang et al. [68], proposed a power management system for a marine sediment microbial fuel cell (MSFC). Over a period of two hours, voltage and current outputs were measured on the MFC while it was subjected to external load. The peak power density was $153\,\mathrm{mW/m^2}$ (normalized by the anode surface area). In comparison with other PMS methods that have been proposed so far, their PMS is larger in size.

In order to supply enough energy for UWSNs to operate with low output power of MFCs, Umaz et al. [69] designed a power system that includes a charge pump, a supercapacitor, and two boost converters. There is a wide dynamic load range of MFCs that can be supported by this system, which results in an end-to-end peak efficiency of 73.185 percent and a relatively short charging time. As a result, their

output can range from 10.89 μW to 108.9 mW under various loads. However, the proposed PMS has not been tested in a real-world environment, but it would be relatively inexpensive.

The authors of [70] propose an inductorless DC-DC (I-DCDC) converter for an energy-aware power management unit (EA-PMU) aimed at harvesting energy from microfluidic cells. In terms of output power, the converter can deliver a wide range of output power, ranging from 7.8 μW (for an MFC load of 8 kΩ) to 1.6 mW (for an MFC load of 100 Ω). 1.6 mW of input power and 1 mA of load current can result in a maximum efficiency of 65%. In terms of implementation costs, this device is relatively inexpensive to implement.

Zhang et al. [71] compared the performance of two MFC PMS designs, the charge pump-capacitor-converter type and the capacitor-transformer-converter type, in supplying power to a wireless sensor network. It is found that capacitor-transformer-converter type PMSs are capable of handling lower input voltages and have shorter charging and discharging cycles. In contrast, PMS that employ charge pump capacitor converters have a slightly higher power efficiency, but are limited in terms of charging and discharging cycles as a result of the presence of the charging pump. Due to its higher efficiency, charge pumps-capacitor-converters are recommended for loads with large duty cycles. However, for missions where the MFC output is low or the charge/discharge cycle is short, it is recommended to use the capacitor-transformer-converter type. Using a minimum input voltage of 0.18 V for capacitor-transformer-converters and 0.3V for charge pump capacitor-converters, they can produce 95 mW of output power.

Authors in [72] describe a system consisting of a MFC and a power management system, which includes a charge pump, a super capacitor, two solid-state switches, and a boost converter. By storing the energy produced by the MFC in a super capacitor, the PMS can provide a burst of power to the load. The proposed system is capable of achieving 95 mW output power and 3.3 output voltage with a minimum input voltage of 0.3 V. Based on the anode surface area of 694cm2, this system is

considered relatively large compared to other works. In terms of cost, it is not too expensive.

2.2.3 Solar Energy

The energy of light can be used to power underwater wireless sensor networks by using solar cells. The method can be applied to surface sonobuoys as well as sensor nodes located near the surface of water at low depths. A low light attenuation makes it ineffective for harvesting solar energy in deep water.

With the use of InGaP (Indium Gallium Phosphide) solar cells, Zayan et al. [73] calculated the amount of energy harvested at different depths in the ocean. Their findings indicated that these types of solar cells have better performance in deeper environments than Tl-based solar cells. At a depth of 5 cm, they are able to harvest 14.42 W/m^2, while at a depth of 5 meters, 5.29 W/m^2r can be harvested.

Amurta et al. [74] have developed a solar-powered water quality monitoring system. A solar panel with an output voltage and power of 13.5V and 1.5W was used by them. During the night, solar cells are unable to produce energy, therefore they developed a 12V battery which stores the output voltage of solar cells. When the output of the solar cells is high during a period of strong light, the battery is put into charging mode by turning on the regulator. Compared to other methods, this method is relatively expensive to implement.

Researchers in [75] submerged two types of solar cells in water in order to determine their performance. They discover that there is a trade-off between the cooling effect for solar cells and the attenuation of light. The harvested voltage for mono-crystalline and poly-crystalline solar cells at the water surface is 6.9V and 4.7V, respectively, and drops to 2.2V and 4V when the distance is 17 cm.

Jenkins et al. [76] experiment high band gap InGaP solar cells for energy harvesting in underwater environment. According to them, the operating voltage of silicon

solar cells drops by 28 percent in depths greater than 2 meters, whereas the performance of InGaP solar cells decreases only by 10 percent. At a maximum depth of 9.1 meters, the output was 0.7 mW/cm (7 Watts per square meter of solar cells).

An underwater monocrystalline solar cell was used by authors in [77] to power an RF modem. During the day, solar cells will supply power to the modems while at night, batteries will provide power to the modems. A battery is charged with a charging current of 1A and 4.2v voltage with solar panels located in water depths of 3m. A modem and energy harvesting component of the system have relatively small dimensions and can be implemented at a low cost.

2.2.4 Seawater Batteries

Seawater batteries are a form of renewable energy that utilizes the oxygen in seawater to provide power to underwater sensor networks. Rechargeable seawater batteries utilize seawater as their cathode material. In order to generate electricity, sodium is harvested from seawater during the charging process, and this sodium is discharged with oxygen dissolved in the seawater, operating as oxidators. Seawater is used as both an anode (Na metal) and cathode (O2) in the proposed rechargeable battery [78]. There is no perfect description of seawater batteries' performance since it depends on the underwater conditions as well as their location [84].

A power management system (PMS) is proposed in [78] as a method for increasing output power of the system as the output voltage of seawater batteries is low, approximately 1.6 volts. Designed to meet the requirements of their application, their PMS can provide 5 and 24 volts.

In their study, Shinohara et al. [79] developed a power harvesting system based on seawater batteries, which can generate an average of 13 Watts over a long period of time. However, the dimensions of their proposed design are too large for underwater sensor networks.

2.2.5 Galvanic Energy

There is also the possibility of harvesting energy from galvanic cells for use by UWSNs. In a galvanic cell, electricity is generated by electrochemistry, with salt in ocean and river water serving as the electrolyte.

Rezaei et al. [80] proposed an energy harvesting method based on galvanic energy. A galvanic cell constructed out of metal strips and mussel shells has been designed by their research team. A maximum voltage of 768 mV can be achieved with this system when there is no load applied. The size of the mussel shell with energy harvesting capabilities is medium.

The authors of [81] attempt to harness underwater energy using galvanic cells. The researchers tested different materials for anodes and cathodes and were able to achieve 1.1 V with graphite-iron as anode and cathode. In terms of size, their proposed method is relatively large for use with underwater sensor nodes.

2.3 Conclusion

As a conclusion, UWSNs can benefit from a wide variety of energy harvesting methods, depending on the network characteristics, such as the amount of energy required to operate the sensors, the location of the nodes, or the size of the underwater network. Kinetic and microbial fuel cells are the most suitable methods of energy harvesting of UWSNs, due to their relatively low cost of implementation, easy implementation and compatibility of their size with sensor nodes. Although these two methods suffer from low outputs, MFCs can use power management systems to increase their outputs. Additionally, underwater sensor networks can benefit from solar power on nodes that are located near the surface and sink nodes. The most incompatible methods with UWSNs are seawater batteries and galvanic cells due to their complexity of implementation and larger size.

Chapter 3

Routing Protocols in Underwater Wireless Sensor Networks

3.1 Introduction

Due to the specific characteristics of the underwater environment and the challenges associated with UWSNs, discussed in chapter 1, routing protocols in terrestrial networks differ from those used in UWSNs. As a result, an underwater routing protocol must provide highly reliable and effective communication links for a network in harsh underwater conditions. It is essential that underwater routing protocols are scalable in order to handle dynamic changes in topology as well as to ensure network stability in times of emergency. Research on underwater networks has received increasing attention in recent years, with many articles related to underwater routing protocols being published [14]–[18]. This chapter will provide a concise overview of the history of routing protocols in UWSNs and briefly highlights recent research in this field.

3.2 Generations of Routing Protocols in UWSNs

3.2.1 First Generation

Initially, UWSN communications were conducted through one hop between the sender and sink, utilizing the long-range properties of acoustic communication. The first generation of routing protocols relied on multi-hop communication through local decisions instead of one hop communications. These protocols were better than one-hop communication as they improved the efficiency of the network. There are several factors that affect the operation of these protocols, such as low density of UWSN deployments, high levels of noise in the aquatic environment, high latency, and poor quality of the underwater acoustic channel. There are several first generation routing protocols, including VBF [18] and FBR [15].

Xie et al. [18] proposed a location-based routing protocol called Vector Based Forwarding (VBF), which requires absolute positioning of nodes. Each data packet in VBF contains the position information of the source node, the forwarder node, and the sink node. A routing vector specifies the data path from the sender node to the destination node. Upon receiving a packet, the node calculates its relative position to the forwarder by measuring the distance between the node and the forwarder, as well as the angle of arrival (AOA) of the signal. If the node was close enough to the routing vector (less than a predefined distance threshold), it updates the packet header and forwards the packet.

Jornet et al. [15] proposed a protocol called FBR (Focused Beam Routing) for networks with both static and mobile nodes. In FBR, each node must know its own location and the location of its final destination, but not the locations of other nodes. A sender node sends a RTS (Request to Send) packet to the network at a minimum power level, and its neighbors respond with a CTS (Clear to Send) packet, indicating that the power level and route are acceptable. Upon failure to receive a CTS, the sender node increases its power level and resends the RTS. Upon receiving CTS, the source is able to determine which node is closest to the destination based on the

node's location and selects the next-hop forwarder node. It is not recommended to use FBR in sparse networks since it consumes more energy and requires a higher transmission power.

3.2.2 Second Generation

In the second generation of routing protocols for UWSNs, geographical routing protocols were introduced. In geographical routing protocols, the most appropriate path is selected based on the node's geographical information (i.e. node's depth or node's specific location). Depth-based or pressure-based routing protocols facilitate selection of the next-hop node and appropriate path based on the node depth information, which is obtained by the pressure sensor on the node.

Routing protocols of the second generation may also implement opportunistic routing (OR). Opportunistic routing involves a set of candidate nodes rather than one forwarder node for advancing the packet towards the destination. In this manner, a packet is transmitted by utilizing the broadcasting nature of wireless communication networks. Candidates that receive packets continue to forward them in a prioritized manner. This means that a low priority node will transmit a packet if no high priority node has done so previously. Consequently, packets are only retransmitted if none of the candidate nodes have received them. Opportunistic routing involves two major procedures: candidate set selection procedure and candidate set coordination procedure.

During the selection procedure for candidate sets, a subset of neighboring nodes is selected to continue forwarding packets to sink nodes. A sender node selects candidates based on their information, which is typically collected through periodic beaconing and a metric or function, such as distance. After selection, candidate nodes are sorted according to their priorities and their ID is included in the packet header.

In candidate set coordination, if the node with the higher priority is unable to forward the message, then the lower priority node can forward it. Consequently, unnecessary and redundant packets, which consume energy, will not be transmitted.

In general, candidate coordination procedures can be divided into two categories: timer-based coordination and control packet-based coordination. In the timer-based coordination procedure, each candidate node holds a packet according to its priority for a certain period of time. A lower priority node suppresses the transmission of the packet during the waiting period if it receives an indication, such as an acknowledgement packet or receipt of the same packet from a higher priority node. As soon as the holding time expires, the packet is forwarded by the node. In control packet-based transmission coordination when a candidate node receives a packet, it responds with a short control packet if none of the high priority candidates respond. Transmission of the control packet serves as a notification to lower priority candidates to suppress their transmissions.

Compared to traditional unicast routing, OR generally increases packet delivery and decreases packet collisions, since at least one candidate is more likely to receive a packet correctly. Nevertheless, packet delivery end-to-end delays are high as a result of the candidate set coordination procedure.

In general, second generation protocols are adversely affected by high delay, high overhead, and void nodes. There are a number of second generation protocols such as DBR [14], HydroCast [85], VAPR [17], GEDAR [16], EnOR [86], etc.

Yan et al. [14] proposed the DBR (Depth-Based Routing for Underwater Sensor Networks) protocol for routing packages based on the depth information of the nodes. Each data packet in this protocol contains a field for storing the depth information of the recent forwarder node. Upon receiving the packet sensor node compares its own depth with the sender's depth. The node will consider itself a qualified candidate if it is located near the water surface. In order to solve the problem of forwarding one packet with multiple nodes and creating multiple paths or

forwarding the same packet repeatedly by one node, authors proposed a packet history buffer and a priority queue. Packets are prioritized by their scheduled sending time, which is dependent on the depth difference between the previous sender and the node.

A hydraulic-pressure-based anycast routing protocol (HydroCast) has been developed by Noh et al. [85] which uses the depth of the sensors to route data to the surface sinks. The HydroCast algorithm selects the next-hop candidate set based on greedy advancement towards the destination. A forwarding set is composed of candidates that are within communication range of one another in order to reduce the hidden terminal problem. A neighboring node that receives the packet will assess its priority on the basis of its proximity to the destination, i.e., the closer to the destination, the higher the priority. A packet will be forwarded by the node if all nodes with a higher priority have failed to send it.

Coutinho et al. [16] proposed geographical routing protocol named GEDAR (GEographic and opportunistic routing with Depth Adjustment-based topology control for communication Recovery). Using greedy opportunistic routing, GEDAR determines the next-hop forwarder set based on the position information of the nodes. As a solution to the problem of void regions, GEDAR proposed a depth adjustment based topology control to move void nodes to new depths as recovery mode.

A lightweight energy-aware opportunistic routing protocol, EnOR, was proposed by Coutinho et al. [86] for achieving balanced energy consumption and increasing the lifetime of UWSN networks. EnOR selects its next-hop forwarding candidate set based on the quality of the link, remaining energy and packet advancement of the neighboring nodes. Additionally, it periodically changes the priority of the candidate nodes depending on their residual energy to increase the lifetime of the network. According to the EnOR protocol, candidates' transmissions are prioritized using timer-based coordination, which assigns each candidate a time slot according to its priority level.

Noh et al. [17] designed a void-aware pressure routing protocol using geographical information for UWSNs named VAPR. The proposed work consists of two major procedures, enhanced beaconing and opportunistic directional data forwarding. In the enhanced beaconing procedure, a node sends beacons containing information regarding its depth, hop count, sequence number, and its current direction of forwarding data (towards the surface). In VAPR, the directional trails are used to perform local opportunistic directional data forwarding. Forwarding decisions are made based on local state variables, data forwarding direction and next-hop data forwarding direction. To avoid the void node problem, the protocol employs a greedy clustering approach based on information about 2-hop connectivity and the distance between neighboring nodes.

Basagni et al. [43] designed an energy-based routing protocol named HyDRO (Harvesting-aware Data ROuting protocol). All nodes in HyDRO have the capability of harvesting energy. A reinforcement learning algorithm was used to select the next candidate node to forward the data based on residual energy, foreseeable harvestable energy in the future, and the quality of the channel. In this protocol, the sensor nodes are considered to be capable of harvesting energy. Nodes deployed at sea bottom or at relevant depths harvest energy through turbines that draw power from sea currents. Nodes located closer to the ocean surface harvest energy by using solar panels mounted on floating devices (e.g., buoys) that are connected to the nodes by cable.

Valerio et al. [44] proposed a Channel-Aware Reinforcement Learning-Based Multi-Path Adaptive Routing protocol named CARMA for UWSNs. According to CARMA, the size and composition of next hop forwarder nodes are dynamic. For each transmission attempt, the protocol uses the RL algorithm to determine the set of next hop relay nodes to optimize route-long energy consumption and packet delivery rates.

Hu et al. [19] developed a machine-learning-based adaptive routing protocol for energy-efficient and lifetime-extended underwater sensor networks (QELAR). In the QELAR protocol, a sender node must include its residual energy, the average

residual energy in its local group, and the value function in the packet header in order to keep its neighbors informed. A Q-learning algorithm is used in QELAR to determine the next forwarder hop, and the reward function is calculated based on the residual energy of the sender node and the distribution of energy among the nodes of the group.

3.2.3 Third Generation

In recent years, routing protocols have been taking advantage of a variety of communication devices at a single underwater node. The nodes are equipped with multiple acoustic modems operating at different frequencies (or programmable modems) or combinations of acoustic and optical modems. The multi-modal multi-hop routing protocols select the most appropriate modem (or physical layer value) at any given moment. Numerous studies have been conducted in this area, including MARLIN-Q [87], CAPTAIN [88], and OMUS [21].

Basagni et al. [87] developed a multi-modal reinforcement learning-based routing protocol, MARLIN-Q, which uses the Q-learning algorithm for selecting the best acoustic modem and next-hop forwarder node. As part of the MARLIN-Q protocol, packets are classified into two classes, urgent and reliable. Priority is given to urgent packets over reliable packets. In order to minimize data delivery delays and packet losses, the cost function for choosing the best forwarder next-hop node and acoustic modem considers the quality of the acoustic channel, packet transmission, and propagation delay.

A routing protocol called CAPTAIN has been proposed by Junior et al. [88] for underwater optical-acoustic sensor networks (UOASNs). To take advantage of the long range of acoustic transmissions and the low energy consumption of optical transmissions, nodes are equipped with both acoustic and optical modems. In this protocol, clusters are created in a network and cluster heads and members are chosen based on their remaining energy and number of their neighbors that can be

reached using optical communications. Afterward, a routing tree is constructed from the sink node to the cluster heads in order to transmit the data. Using cluster heads, data is gathered by them, aggregated, and then passed to their next hop to reduce the amount of network traffic. Nodes within the cluster communicate via optical communication, while cluster heads communicate via acoustic communication with one another and the sink.

Coutinho et al. [21] proposed an opportunistic routing protocol in Multi-Modal Underwater Sensor Networks named OMUS. In this protocol, each node is equipped with a number of acoustic modems that have various settings. The goal of OMUS is to select the best modem and best next-hop candidate set jointly in order to enhance the data delivery and energy consumption. Two heuristics are proposed, OMUS-D and OMUS-E. OMUS-E selects next hop forwarder candidate nodes and appropriate acoustic modem that reduce energy consumption. In the OMUS-D heuristic, selection is based on increasing the probability of one-hop data delivery.

An overview of discussed routing protocols is provided in table 3.1.

TABLE 3.1: Summary of Routing Protocols

Protocol (Year)	**Method**	**Energy Efficiency**	**Reliability**	**Energy Harvesting**
VBF (2006) [18]	Routing vector based on position of the node	✓	✓	
FBR (2008) [15]	Select next-hop node based on location of the node	✓	✓	
DBR (2008) [14]	Select next-hope node based on depth information	✓	✓	
HydroCast (2015) [85]	Select next-hope forwarder set based on depth information	✓	✓	
GEDAR (2014) [16]	Use OR to select next-hope forwarder set based on the position information	✓	✓	

Table 3.1 – *Continued from previous page*

Protocol (Year)	**Method**	**Energy Efficiency**	**Reliability**	**Energy Harvesting**
EnOR (2017) [86]	selects the next-hop forwarding candidate set based on the quality of the link, remaining energy and packet advancement of the neighboring nodes	✓	✓	
VAPR (2012) [17]	Use OR to select next-hop forwarder node based on data forwarding direction	✓	✓	
HyDRO (2018) [43]	Use RL to select next-hope candidate node based on residual energy, harvestable energy in the future, and channel quality	✓	✓	✓
CARMA (2019) [44]	Use RL to select next-hope candidate set to optimize route-long energy consumption and packet delivery rates	✓	✓	
QELAR (2010) [19]	use Q-learning to select next forwarder hop based on the residual energy of the sender node and the distribution of energy among the nodes of the group	✓	✓	
MARLINQ (2019) [87]	Use QL to select best acoustic modem and next-hop forwarder node based on quality of channel, packet transmission rate and propogation delay	✓	✓	
CAPTAIN (2020) [88]	Use clustering and acoustic and optical modem to transfer the data	✓	✓	
OMUS (2021) [21]	Use OR to choose best acoustic modem and set of candidate nodes based on reducing energy consumption and data delivery rate	✓	✓	

Nevertheless, energy harvesting has been overlooked in underwater sensor networks. Han et al. [89] developed an analytical framework to study the throughput of underwater nodes in scenarios where the number of nodes ready for data communication varies because nodes harvest energy from tidal currents. Wang et al. [90] modeled the optimal transmission power allocation problem at relay nodes with energy harvesting capabilities, aimed at maximizing the sum of the data rate over N time-slots. Guida et al. [84] designed an underwater sensor node that can be recharged wirelessly through ultrasonic waves. In their considered scenarios, underwater sensor nodes are wireless powered through acoustic waves emitted by ships, buoys, or underwater devices (e.g., remotely operated vehicles - ROVs or unmanned underwater vehicles - UUVs). In the designed node, an energy management unit is responsible for receiving, converting, and storing energy.

3.3 Conclusion

In conclusion, three generations of routing protocols were discussed in the chapter. First generation routing protocols used multihop communication between nodes instead of one hop communication from sender to sink, as well as a single node as the next-hop forwarder node. The second generation of routing introduced opportunistic routing as well as routing based on geographical information. As part of the OR protocols, a set of candidate nodes was selected to serve as next hop forwarders. In the third generation of protocols, multi-modal multi-hop protocols, a variety of communication devices are utilized at a single underwater node. In these protocols, the most appropriate modem (or physical layer value) is selected at any given time.

Additionally, to the best of our knowledge, networking protocols designed for UWSNs have neglected the energy harvesting mechanisms that can be used in underwater sensor nodes. For instance, there is no opportunistic routing (OR) protocol with set of forwarder candidate nodes that explores the energy harvesting capabilities of underwater sensor nodes to achieve high data delivery reliability while

prolonging the UWSN lifetime.

Chapter 4

The Proposed RELOR Protocol

4.1 Introduction

The RELOR protocol is the first opportunistic routing protocol that explores the energy harvesting capabilities of underwater sensor nodes to determine energy-efficient and reliable routing paths in UWSNs. The proposed protocol implements a reinforcement learning mechanism for the next-hop forwarder set selection, which allows underwater sensor nodes to learn how to route data packets through energy-efficient and high-reliable multi-hop routing paths. The protocol consists of two major procedures, namely the candidate set selection procedure and the data transmission coordination procedure.

In this chapter, the candidate set selection procedure is presented in section 4.2, section 4.3 discussed the data transmission procedure implemented by the RELOR protocol, and section 4.4 concludes the chapter with a brief summary.

4.2 RELOR's candidate set selection procedure

In the RELOR protocol, candidate nodes are selected based on the expected energy cost of the routing path to deliver the packet to the surface sonobuoy, which accounts for the link quality, energy cost per transmission, and the expected energy cost of the next hop forwarder nodes. The general goal at each hop is to select a set of next-hop forwarder nodes that would minimize the energy cost to deliver

the packet. Herein, there is a trade-off to be considered when selecting next-hop forwarder nodes. A large set of next-hop forwarder nodes reduces packet retransmissions since a data packet is lost and needs to be retransmitted only if none of the candidate nodes received it. This reduces the energy cost at the hop. Nevertheless, a large set of next-hop forwarder candidate nodes increase the complexity of coordinating the transmissions of the candidate nodes and might increase the hidden terminal problem, which results in redundant data transmissions, packet collisions, and energy waste. The overall goal is to select a set of next-hop forwarder candidate nodes at each hop that is large enough to guarantee an energy-efficient and highly reliable data delivery at the hop, without wasting energy. The RELOR protocol addresses this challenge by considering the link quality, energy cost, and harvestable energy when selecting candidate nodes.

4.2.1 Periodic beaconing procedure

The RELOR routing protocol implements a procedure for periodic beaconing. In the RELOR protocol, the periodic beaconing is used by underwater sensor nodes to obtain information about the one-hop neighborhood, determine the link quality for the neighbors, and obtain the energy cost for data delivery from the neighbor to the surface sonobuoy. In this sense, a beacon packet has the following fields: sender's unique identifier, the number of packets the sender has transmitted, and the sender's expected energy cost for data delivery, i.e., the expected energy cost of the routing path to successfully deliver the packet the surface sonobuoy. The RELOR's periodic beaconing procedure is presented in Algorithm 1. At the time of a beacon transmission, a node will create a beacon packet (Line 1), add its unique address in the packet header (Line 2), and the number of packets it has transmitted including the current transmission (Line 3). Hence, the node adds its expected energy cost to successfully deliver the packet to the next-hop forwarder nodes (Line 4) and, finally, broadcast the beacon packet (Line 5). The node also reschedules the

transmission of its next beacon packet (Line 6). If not otherwise specified, each underwater sensor node transmits a beacon packet every 120 seconds.

Algorithm 1 RELOR's Periodic Beaconing Procedure

1: b: a new beacon packet
2: $b.saddr \leftarrow sender.id$
3: $b.numtransmissions \leftarrow ++numberoftransmissions$
4: $b.deliverycost \leftarrow e_c^i$
5: Broadcast b
6: Reschedule next beacon transmission

In Algorithm 1, e_c^i is the expected energy cost to deliver the data packet to the next-hop forwarder nodes. This cost is calculated as follows. First of all, e_c^i will be 0 if the beacon sender is the surface sonobuoy. If the beacon sender i is an underwater sensor node and it does not know about any neighbor, i.e., its neighbor table is empty, its cost is set to infinity; if it has only one neighboring node j, its expected energy cost to deliver the data packet to the next-hop candidate nodes is:

$$e_c^i = min\left(K, \frac{1}{p_{i,j}}\right) \times \frac{L}{B} e_T + e_c^j \tag{4.1}$$

where K is the maximum number of trials to deliver a data packet, $p_{i,j}$ is the quality of the link between the node i and its neighbor j, L bits is the size of the data packet, B bps is the data rate, e_T Watts is the transmission power, and e_c^i is the expected energy cost of the neighbor j.

In the case where the current sender node i has more than one neighbor, i.e., $|N_i|>1$, the expected energy cost of node i to deliver the packet is calculated from the i's expected energy cost to deliver the packet to its next-hop forwarder candidate nodes and from the expected data delivery energy cost from each candidate node. Hence, the $C_i^k \subseteq N_i$ is defined as the set of next-hop forwarder candidate nodes of node i for its k th trial of delivering the packet (see Section 4.1.3), where $k = 0, 1, ..., K-1$. The candidate set C_i^k is sorted in a descending manner based on the

priorities of the selected candidate nodes, i.e., $n_j > n_l$ means that the neighbor at the j^{th} location in the set C_i^k has higher forwarding priority than the neighbor at the l^{th}, and the l^{th} candidate in the set i's candidate set C_i^k only forwards i's transmitted data packet if the j^{th} neighbor in the candidate set failed to do so. Therefore, the node i's expected energy cost to deliver the packet is calculated as:

$$e_c^i = \sum_{k=0}^{K-1} \left\{ \left(\prod_{m=0}^{k-1} P_f^m \right) \times \left[1 - \prod_{j=1}^{|C_i^k|} \left(1 - p_{i,n_j} \right) \right] \times \left[\frac{L}{B} e_T + \prod_{j=1}^{|C_i^k|} p_{i,n_j} \left(\prod_{l=0}^{j-1} 1 - p_{i,n_l} \right) \times e_c^{n_j} \right] \right\} \tag{4.2}$$

where P_f^m is the probability of transmission failure, i.e., packet not delivered, at the transmission trial m, which is given as $P_f^m = \prod_{j=1}^{|C_i^m|} \left(1 - p_{i,n_j}\right)$. In Eq. 4.2, p_{i,n_0} is defined as 0 and P_f^0 is defined as 1 for ease of notation.

4.2.2 RELOR's RL-based forwarders set selection procedure

One of the key components of the RELOR protocol is the reinforcement learning (RL) procedure implemented to select next-hop forwarder candidate nodes. By using Reinforcement Learning (RL), a system can learn how to accomplish a goal in control problems based on its previous experience. RL agents choose their actions based on the current state of the system and the reinforcement they receive from the environment. RL algorithms are commonly based on estimating value functions, state-action pairs, which assess what it means for an agent to be in a given state (or to perform an action in a given state). The framework for RL is depicted in Figure 4.1.

The general idea of the proposed next-hop forwarder candidate set selection procedure is to make a node i capable of learning the best decision, i.e., the selection of next-hop forwarder nodes, from its neighborhood information channel quality, neighbors' expected energy cost to deliver the packet, data delivery attempts, and neighbors' foreseeable harvested energy.

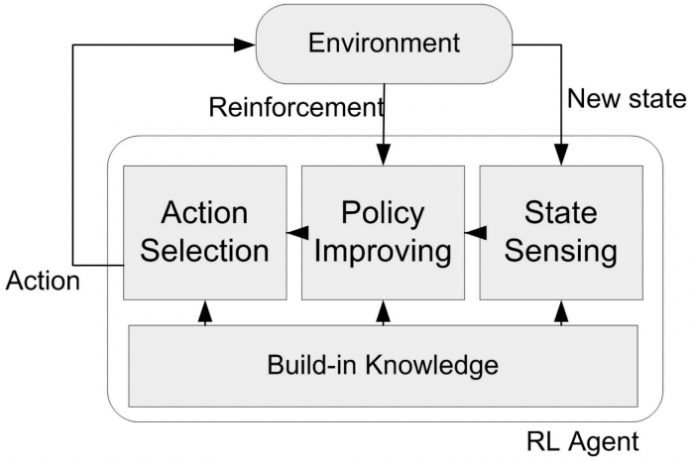

FIGURE 4.1: The framework of reinforcement learning [19]

Herein, the next-hop candidate set selection problem is modeled by a Markov decision process (MDP). An MDP model consists of (S, A, P, C) tuples, where S is the set of states, A is the set of possible actions, P is the state transition probability, and C is a cost function. Similar to [43], we model the set of states of a node i from the possible number of transmission attempts the node will have to deliver the data packet to its next-hop nodes. Hence, we define the set of states as:

$$S = \{0, \ldots, K-1, rcv, drop\}, \tag{4.3}$$

where $0 \leq k \leq K-1$ represents the number of times the node already attempted to deliver the data, rcv represents the successful reception of the data packet by at least one of the next-hop forwarder candidate nodes, and $drop$ represents the failure of delivering the data packet to the next-hop forwarder nodes during the maximum K attempts.

If the state $s = rcv$ or $s = drop$ is observed, no action is needed, i.e., $A_i(s = rcv) = A_i(s = drop) = \emptyset$. Otherwise, a node i will make a decision of selecting its next-hop forwarder candidate set C_i^s. To do so, neighboring nodes at N_i are sorted in an increased manner based on their energy cost. That is, for $N_i = \{n_1, n_2, n_3\}$, for instance, the expected energy cost of the node i's neighbors, estimated from Eq. 4.1 or Eq. 4.2, is $e_c^{n_1} < e_c^{n_2} < e_c^{n_3}$. In the RELOR protocol, the neighbor with the lowest

expected energy cost to deliver the data packet is always added to the forwarding candidate set. Next, additional neighbors are considered and they might be added or not in the candidate set. Therefore, the set of possible actions at a state s is defined as:

$$A_i(s) = \{1\} \times \{0,1\}^{|N_i|-1} \tag{4.4}$$

Herein, we define the parameter σ that is used when just the σ^{th} first neighbors in the sorted set $N(i)$ must be considered rather than all sets of neighbors. This parameter can be used to control the size of A_i and reduce the computation cost to determine the optimal action. Let us assume that a node n_i is at the state $s = 0$ and has three neighbors, i.e., $N_i = \{n_1, n_2, n_3\}$. The set of possible actions it can take and its resulting candidate set are presented below:

- $a = 100, \quad C_i^0 = \{n_1\};$
- $a = 110, \quad C_i^0 = \{n_1, n_2\};$
- $a = 101, \quad C_i^0 = \{n_1, n_3\};$
- $a = 111, \quad C_i^0 = \{n_1, n_2, n_3\}.$

Next-hop forwarder candidate sets with a large number of nodes might not be desired since it can increase the complexity and energy cost for transmissions coordination. Herein, the maximum size of a candidate set might have is a parameter, σ, in the RELOR protocol. We have set σ as 5 unless otherwise specified. Hence, at a given node i, the RELOR protocol only considers the σ most well-ranked neighbors when determining the next-hop forwarder candidate set for the node i.

The transition probability between successive states s and s' depends on the current state s and on the action $a \in A_i(s)$ taken by the node i, and is given as:

$$P^{a}_{i,s\to s'} = \begin{cases} 1 - p_J(s), & \text{for } s \leq K-2, s' = s+1 \\ 1 - p_J(s), & \text{for } s = K-1, s' = drop \\ p_J(s), & \text{for } s \leq K-1, s' = rcv \\ 0, & \text{otherwise.} \end{cases} \tag{4.5}$$

In Eq. 4.5, $p_J(s)$ is the probability that at least one of the candidate nodes in the selected candidate set C_i^s successfully received the transmitted data packet from node i at its attempt s to deliver the packet. This probability is estimated as:

$$p_J(s) = 1 - \prod_{j=1}^{|C_i^s|} \Big(1 - p_{i,n_j}\Big). \tag{4.6}$$

Finally, we define the cost function that determines the cost incurred at each state $s \in S$ when the node selects the action $a \in A_i(s)$. This cost function will drive the optimized selection of the set of candidate nodes at each node. The cost function can be defined in Eq. 7. In Eq. 7, p_{i,n_0} is defined as 0 for ease of notation, e_H is the energy harvesting rate at each underwater sensor node, and F_{p_J} is an energy penalty associated with the action $a(K-1)$ of the last retransmission of the packet, where F is set to an arbitrarily high value. As in [43], this penalty aims at discouraging node i to drop the packet.

$$c_i(s,a) = \begin{cases} \Big[\frac{L}{B}e_T + \sum_{j=1}^{|C_i^s|} e_c^j p_{i,n_j} \times \prod_{k=0}^{j-1}(1 - p_{i,n_k})\Big] - e_H, & \text{if } s = 0 \\ \Big[(s+1)\frac{L}{B}e_T + \sum_{j=1}^{|C_i^s|} e_c^j p_{i,n_j} \times \prod_{k=0}^{j-1}(1 - p_{i,n_k})\Big], & \text{if } 0 < s < K-1 \\ F p_J(K-1), & \text{if } s = K-1. \end{cases} \tag{4.7}$$

RELOR uses the Q-Learning algorithm to solve the devised MDP model and

Algorithm 2 SELECTCANDIDATENODES(k)

1: **for all** episode **do**
2: Select initial state $s = 0 \in S$
3: **repeat**
4: Judge the next state $s' \in S$ according to the selected action
5: Select maximum Q-value for next state based on all possible actions by looking up Q-table method
6: Update Q-value for current state s by Eq. 4.7
7: Set the next state s' as the current state
8: **until** current state is different from *rcv* and *drop*
9: **end for**
10: $action \leftarrow arg\,min_{a \in A_i(k)} Q_i(k, a)$
11: $C_i^k \leftarrow$ DETERMINECANDIDATENODES(action)
12: **return** C_i^k

determine the action, i.e., candidate nodes, for each state at each underwater sensor node. First of all, each node i starts with no knowledge about its environment, i.e., neighbors and links quality. It acquires the one-hop neighborhood information through the beaconing procedure discussed in Section 4.1.2. The periodically acquired one-hop neighborhood information is used to update the value function V_i and transition probabilities $P^a_{i,s \to s'}$ at each node i. Algorithm 2 presents the Q-Learning procedure implemented by the RELOR routing protocol to enable underwater sensor nodes to learn energy-efficient and reliable multi-hop paths to the surface sonobuoy. The obtained action for each state (Line 10) is used to determine what is the subset of the node i's neighboring nodes (Line 11) that will be the next-hop candidate nodes for the data packet that is being transmitted at the k^{th} attempt. Given an action $a \in \{1\} \times \{0, 1\}^{n-1}$, 1 means that the neighboring node at the corresponding location in the neighbor set is selected as candidate node, and 0 means the contrary.

4.3 RELOR's data transmission procedure

The RELOR routing protocol implements a straight forward procedure for data transmission. This procedure is presented in Algorithm 3. Whenever a node i has a data packet to transmit, which can be a data packet that it produced or a received packet that it needs to forward, it first of all includes in the packet header the number of packets it has transmitted (Line 1). This information is used by the receiver nodes to estimate the link quality to the sender i. Next, the node will attempt up to K times to successfully deliver the packet to its next-hop nodes. The next-hop nodes of a node i will depend on what it has learned about the environment. In case i has only one neighbor, it selects the neighbor as next-hop forwarder node (Line 5). In case it has more than one neighbor, it will select a set of next-hop forwarder candidate nodes as discussed in Section 4.1.3. Finally, a node i will simply broadcast its data packet if it does not known any neighbor (Line 10). A node will stop its attempt to deliver a data packet to the next-hop nodes if it reaches the K maximum number of triefs or if it receives an acknowledgment packet from one of the candidate nodes (Lines 13-15).

4.3.1 RELOR's transmission coordination procedure

The acknowledgment (ACK) packet is also used to coordinate the transmission of next-hop forwarder candidate nodes. An ACK packet is sent when a higher priority node receives the packet. Candidate nodes with lower priority will disregard the data packet upon receiving ACK from higher priority nodes. RELOR implements a timer-based transmission prioritization among candidate nodes. Hence, the higher is the transmission priority of the candidate node, the lower is the amount of time it will hold the received data packet before transmitting it. The packet holding time at candidate nodes is given by:

$$h_p = \pi_j \frac{D}{v}, \tag{4.8}$$

Algorithm 3 TRANSMITDATA(P)

1: $p.atp \leftarrow ++ amount\_of\_transmitted\_packets$
2: $k = 0$
3: **while** $k < K$ **do**
4: **if** *There is one known neighbor j* **then**
5: *forward the packet to j*
6: **else if** *There are more than one known neighbor* **then**
7: $\mathcal{C}_i^k \leftarrow$ CANDIDATESETSELECTION(k)
8: *forward the packet to* $\mathcal{C}_i^k$
9: **else**
10: BROADCAST(p)
11: **end if**
12: $k \leftarrow k + 1$
13: **if** *An ACK for the packet is received within* τ *time units* **then**
14: break
15: **end if**
16: **end while**
17: *discard packet*

where π_i is the forwarding priority of the candidate node j, D is defined as a safe range, and $v = 1500m/s$ is the approximate sound propagation speed. In other words, D/vs in Eq. 4.8 estimates the amount of time that a transmitted packet would take to be propagated over distance D. This is to guarantee that all nodes within the distance D of the forwarder node will be able to hear the transmission of the high priority forwarder node and cancel its rescheduled transmission of the same packet.

The parameter D will impact data delivery reliability, energy cost, and end-to-end delay. The higher is the value of D, the fewer is the redundant data transmissions will incur, which would reduce the overhead in the acoustic channel, packet collisions, and unnecessary energy consumption. However, it will increase the end-to-end delay for data delivery. Herein, unless otherwise specified, D is set to 600 m. A more efficient approach is to set D adaptively, considering the network traffic

load.

Whenever a node receives a data packet, it broadcasts an ACK packet to indicate that it has successfully received the data packet. As mentioned in Section 4.1.4, upon the reception of the ACK, the sender node will cancel rescheduled retransmissions of the data packet. Besides, low priority candidate nodes will cancel their scheduled transmission of the packet that was successfully received and acknowledged by the highest priority candidate node

4.4 Conclusion

This chapter proposed the RELOR protocol, which is a novel reinforcement learning-based OR protocol that considered the foreseeable energy to be harvested in the neighboring nodes, the energy cost, and link quality to select the set of next-hop candidate nodes at each hop. RELOR protocol has two major procedures, candidate set selection procedure and data transmission procedure.

Chapter 5

Performance Evaluation

In this chapter, we conduct extensive simulations to evaluate the performance of the proposed RELOR routing protocol. We use the HyDRO [43] and CARMA [44] routing protocols as baseline when evaluating the performance of the RELOR protocol. HyDRO is the first routing protocol for UWSNs that considered the energy harvesting capability of underwater sensor nodes when selecting a next-hop node at each hop. However, the HyDRO routing protocol selects a single next-hop node at each hop, instead of a subset of next-hop forwarder nodes. In CARMA next forwarder nodes set are selected based on route-long energy optimization. Similar to the proposed protocol, CARMA chooses a set of candidates to forward the data, but it does not take into account the capabilities of the nodes to harvest energy.

We compare the performance of the RELOR, HyDRO and CARMA routing protocols in terms of packet delivery ratio, which is the fraction of produced data packets that are successfully delivered to the surface sonobuoy, average end-to-end delay, which is the average delay in the network to deliver a produced data packet, number of duplicated received packets, which is the number of packets that are received with more than one sink, network energy consumption, which is the total amount of the consumed energy of the underwater sensor nodes, and node energy consumption which is the amount of the consumed energy by each node.

TABLE 5.1: Simulation parameters

Parameter	Value
`Simulation duration`	3 h
`Number of nodes`	[15, 40]
`Number of surface sonobuoys`	1, 3
`Size of the deployment area`	4 km × 2 km × 240 m
`Location of the surface sonobuoy`	(2000, 1000, 10) (1000, 500, 10) (3000, 1500, 10)
`Initial energy`	80 kJ
`Modem Tx power`	8.5 W
`Modem Rx power`	0.5 W
`Modem idle power`	0.285 W
`Energy harvesting rate`	95 mW
`MAC protocol`	CSMA-ALOHA
`Packet payload size`	1000 B
`Packet inter-generation time`	{10, 30, 60, 100} s
`TTL neighbor entry`	900 s
`Maximum number of retransmissions`	K=4
`Number of replications`	30
`Discount factor` γ	0.95
`Safe range D`	600 m

5.1 Simulation Scenarios

We use the DESERT underwater simulator [45], [46] to implement those protocols. The DESERT Underwater is a comprehensive tool for the simulation and emulation of underwater network experimentation. It considers the peculiar characteristics of the underwater acoustic channel, underwater sensor networks, and underwater environment, which enables one to conduct realistic simulations of UWSN applications. In this study, we consider an area of interest of 4 km × 2 km and depth of 240m. We simulate the random deployment of a variable number of underwater sensor nodes, ranging from 15 to 40, according to a uniform distribution. Three surface sonobuoys are deployed at the surface of the area of interest and their acoustic modems are at depth of 10 m. Fig. 5.1 illustrates the position of three sinks on the surface of the network.

In the simulations, underwater nodes communicate through an acoustic modem

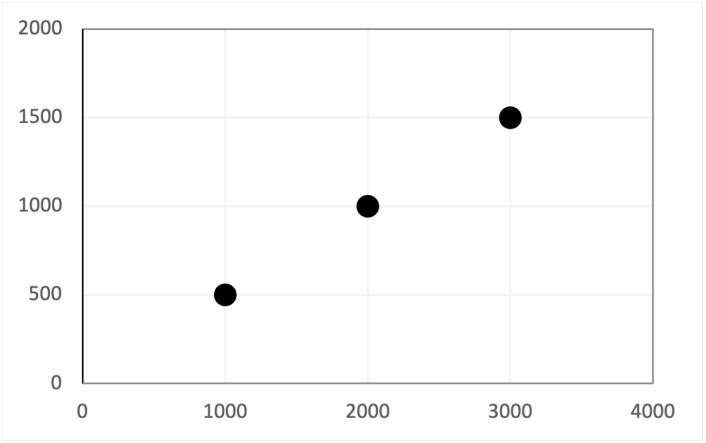

FIGURE 5.1: Position of 3 Sinks in the Network's Surface

whose carrier frequency is set to 25.6 kHz for a bandwidth of 4 kHz, resulting in a bit rate of 4000 b/s. The transmission, reception and idle powers of the acoustic modem are set to 8.5 W, 0.5 W, and 0.285 W, respectively. These considered values are consistent with commercial acoustic modems (e.g., Teledyne Benthos DAT [91] and Evologics [92]) and the parametrization considered in [43]. Furthermore, we assume each node is equipped with a rechargeable battery packet, whose initial energy is 80 kJ, with microbial fuel cells connected in series that harvest energy from certain electrochemical reactions and bacteria existing in the water, at a rate of 95 mW [72]. Finally, we consider that data packets are generated at fixed time intervals. Once a data packet is generated, it is associated with a source randomly and uniformly selected among all underwater sensor nodes. We considered different packet inter-generation time of 10, 30, 60, and 100 seconds. The remaining parameters are presented in Table 5.1. The results represent the average value of 30 replications and a confidence interval of 95%.

5.2 Performance Results

Fig. 5.2 shows the packet delivery ratio for packet inter-generation time of 10 s, 30 s, 60 s and 100 s, and varied number of underwater sensor nodes. The first trend is that the proposed RELOR protocol outperforms HyDRO and CARMA in all considered

scenarios of traffic load and network density. For the heavy traffic load scenarios, i.e., packet inter-generation time of 10 s, RELOR showed an increased perceptual of 100 % in the packet delivery ratio, as compared to both protocols. The percentage gain is even higher for low traffic load scenarios. RELOR presents better performance because it selects a subset of neighboring nodes at each hop, and the selected nodes will collaborate to advance the packet towards the destination, while also taking into account how much energy can be harvested in advance for a longer network life-time.

In contrast, the HyDRO protocol selects a single next-hop node, which is the best neighbor mostly in terms of residual energy. HyDRO's diminished performance is because of poor link quality from the sender to the selected single next-hop node and lack of backup forwarder node. On the other hand, the CARMA protocol selects a subset of forwarding candidate nodes similar to the RELOR protocol, but does not take into consideration the energy harvesting capabilities of sensor nodes. The CARMA protocol also does not take residual energy into account when choosing forwarder candidate nodes, and it does not have a procedure for removing dead nodes (i.e., those whose energy is zero). In high traffic areas of the sensor network, this leads to nodes consuming an excessive amount of energy and becoming dead, resulting in low performance of the protocol.

Another trend observed in Fig. 5.2 is that the higher is the packet inter-generation time, the higher is the packet delivery ratio for all protocols. This is because fewer packets are transmitted in the network, which reduces packet collision and losses. RELOR's packet delivery ratio is 50% lower in high traffic load as compared to scenarios of low traffic load. Such decrease is not observed in the HyDRO protocol, as it suffers more from the poor link quality from the sender node to its selected next-hop node at each hop.

Fig. 5.3 depicts the average end-to-end delay. As expected, the data delivery delay in RELOR is higher when the traffic load is high. As the traffic load decreases,

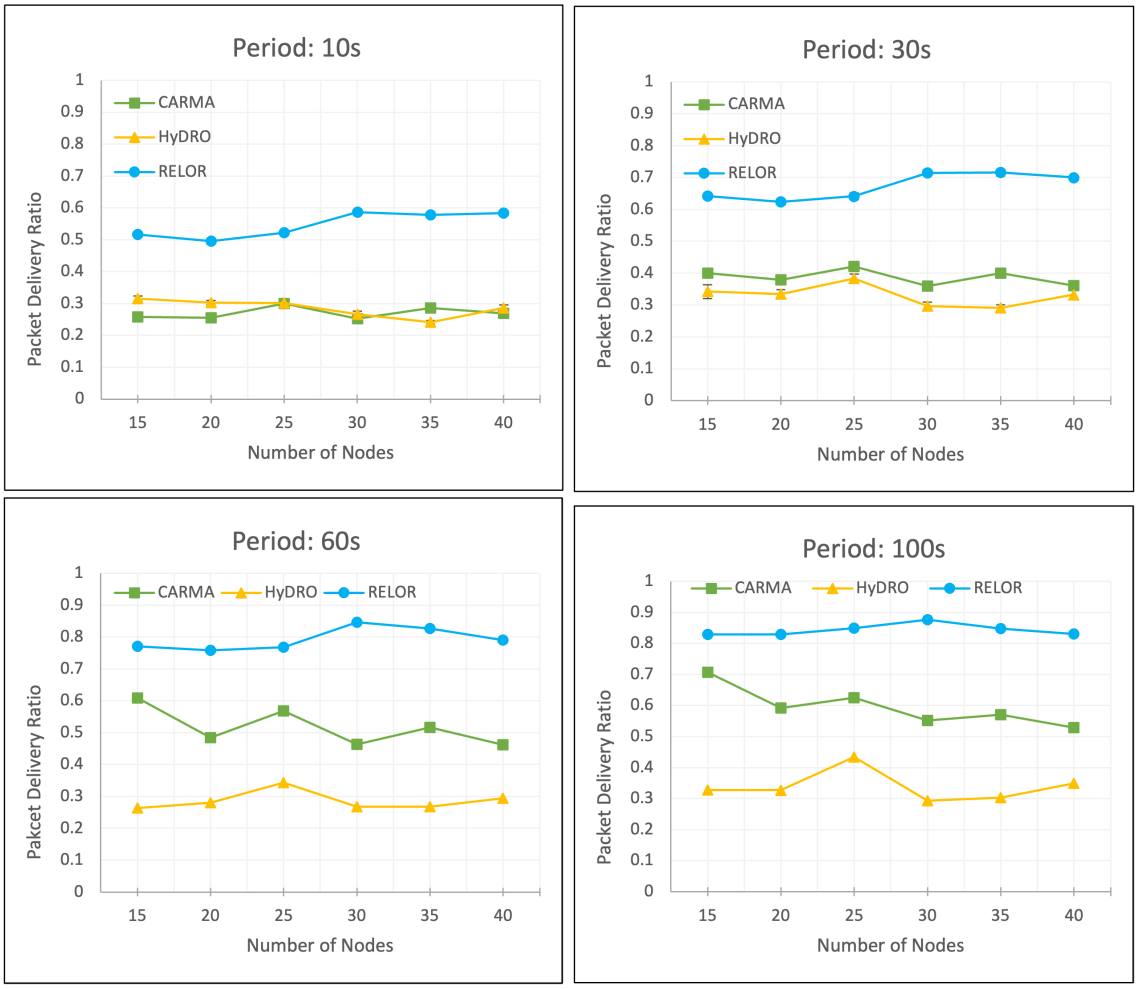

FIGURE 5.2: Packet Delivery Ratio

the end-to-end delay decreases. This is because of packet collisions and retransmissions, as more packets need to be delivered. Moreover, RELOR implements a priority-based function for the transmission coordination among candidate nodes. Thus, the lower is the priority of the candidate node, the higher is the amount of time it will hold the packet before transmitting it. In scenarios of high traffic load, high-priority candidate nodes might not receive the data packet due to collisions. Hence, low priority nodes will be the ones to forward it, which will increase the delay the packet will experience. This is corroborated by the fact that the delay in the RELOR protocol is 83 % higher than in the HyDRO protocol for scenarios of low network density and high traffic load. RELOR protocol has a similar average end-to-end delay as the CARMA protocol. This is due to the fact that CARMA protocol chooses the next-hop forwarder node at every transmission attempt, which results

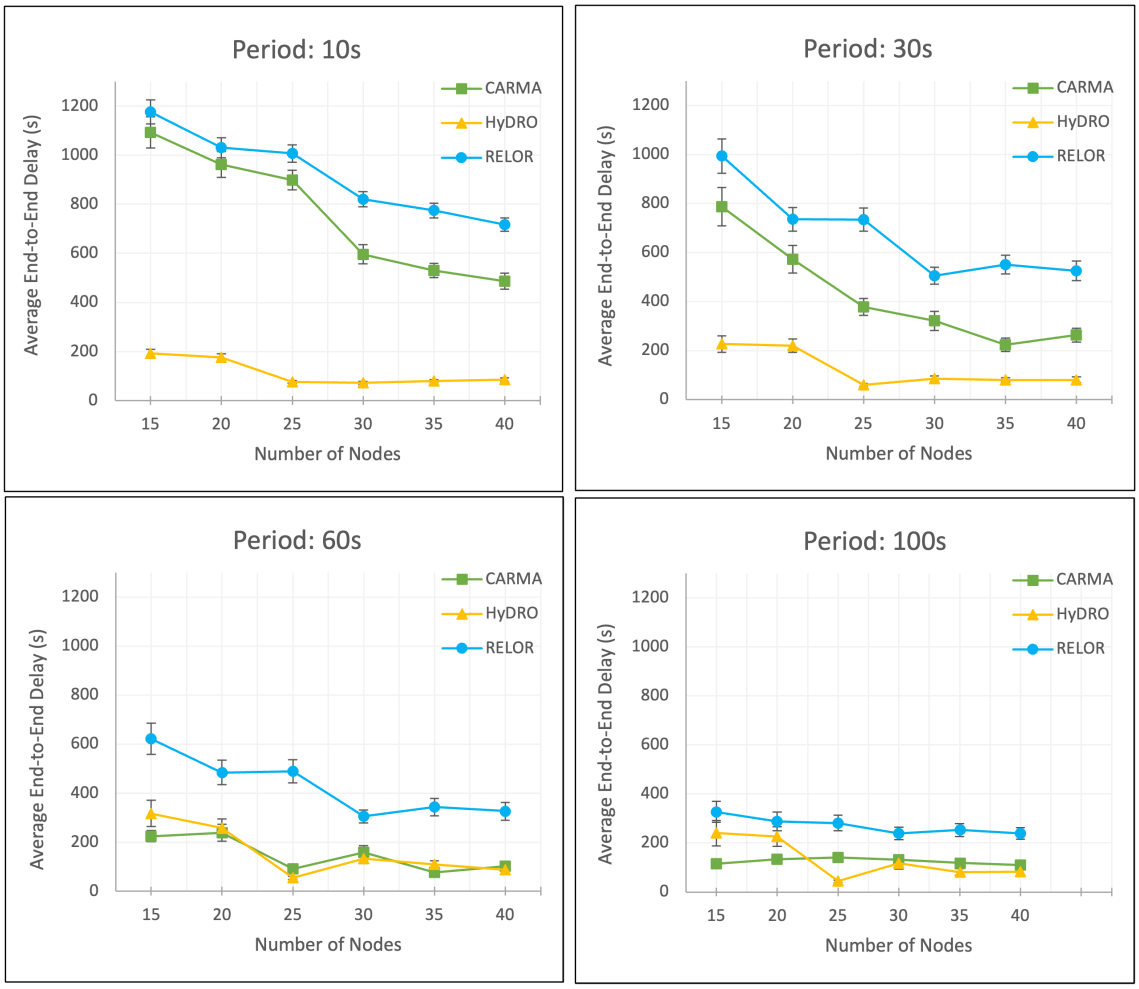

FIGURE 5.3: Average End-to-End Delay (s)

in a greater end-to-end delay. As the traffic load decreases, the end-to-end delay in the RELOR protocol decreases. This expected trend is because of more availability of the channel and fewer packet collisions and retransmissions. RELOR experiences approximately the same delay as two other protocols in the scenario with a period of 100 seconds.

Fig. 5.4 shows the number of duplicate packets that have been received by the sinks. The fact that the network has three sinks makes it possible for some packets to be received by more than one sink. The number of duplicated packets is higher in high traffic scenarios as they produce more packets.

Figs. 5.5 and 5.6 portray the network's total energy consumption for the scenarios of 15 and 40 underwater sensor nodes, respectively. Overall, the average energy

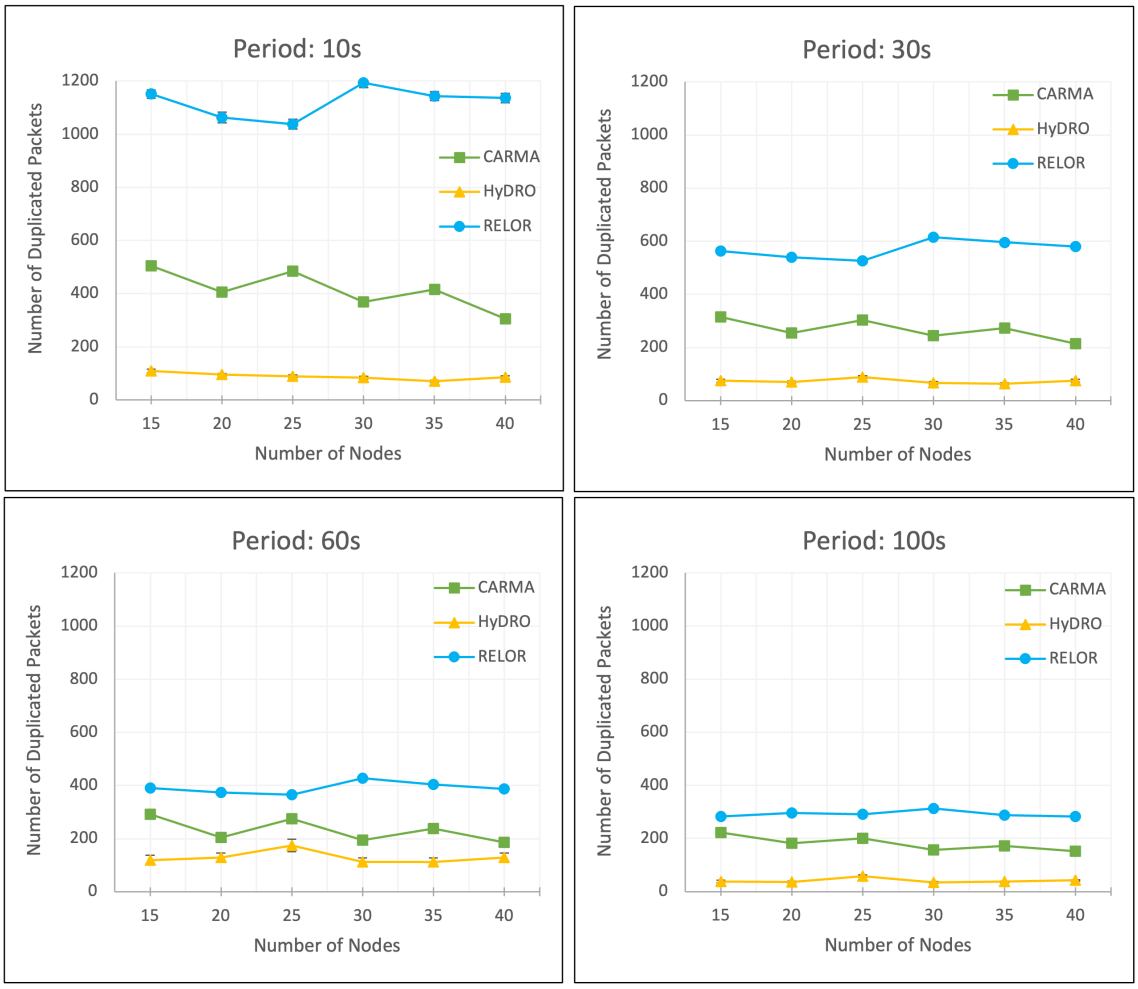

FIGURE 5.4: Number of Duplicated Received Packets

consumption in the RELOR protocol is lower than in the HyDRO and CARMA, although more packets are successfully delivered (Fig. 5.2). In both scenarios (low network density and high network density) even the highest energy consumption in RELOR is comparable to the lowest energy consumption in two other protocols. This is because a packet is lost and needs to be retransmitted only if all next-hop forwarder nodes, in each hop, failed to receive it. In contrast, the HyDRO protocol needs to retransmit a data packet if the selected next-hop node failed to receive it either because of the poor link quality or packet collision, which is expensive in terms of energy cost since the cost to transmit a data packet is of the order of tens of Watts. In CARMA protocol, next hop forwarder sets are not selected based on their cost efficiency, causing higher energy consumption.

Fig. 5.7 and Fig. 5.8 illustrate the nodes' energy consumption in a network for

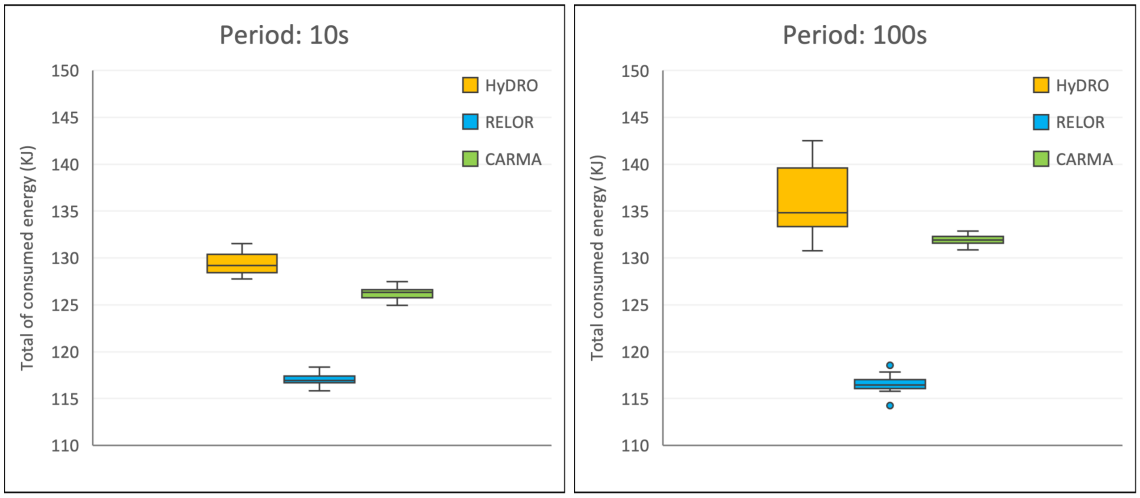

FIGURE 5.5: Total Network Energy Consumption. Scenario of 15 Nodes.

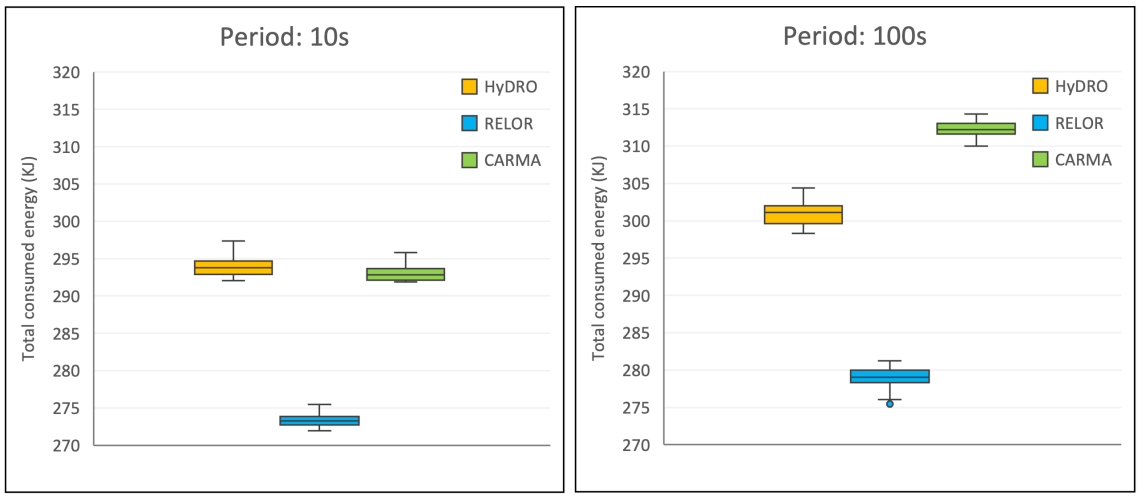

FIGURE 5.6: Total Network Energy Consumption. Scenario of 40 Nodes.

15 and 40 nodes in low and high traffic networks, respectively. There is a decrease in the energy consumption of the nodes in RELOR compared to 2 other protocols. In the scenario with 40 nodes, the highest node energy consumption in RELOR is even lower than the lowest node energy consumption in CARMA and HyDRO, due to the same reasons detailed in Fig. 5.5 and Fig. 5.6. Furthermore, the results show the overuse of a few nodes in the HyDRO routing protocol. Those outline nodes, in terms of energy consumption, are highly demanded during multi-hop data routing. Such overuse of a few nodes will drain their batteries quickly and result in network partitions.

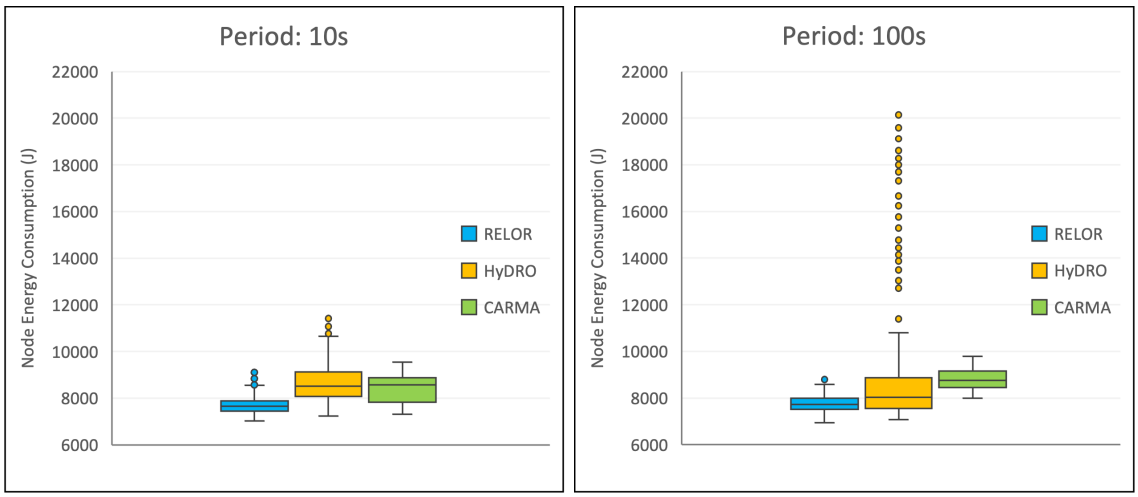

FIGURE 5.7: Average Node Energy Consumption. Scenario of 15 Nodes.

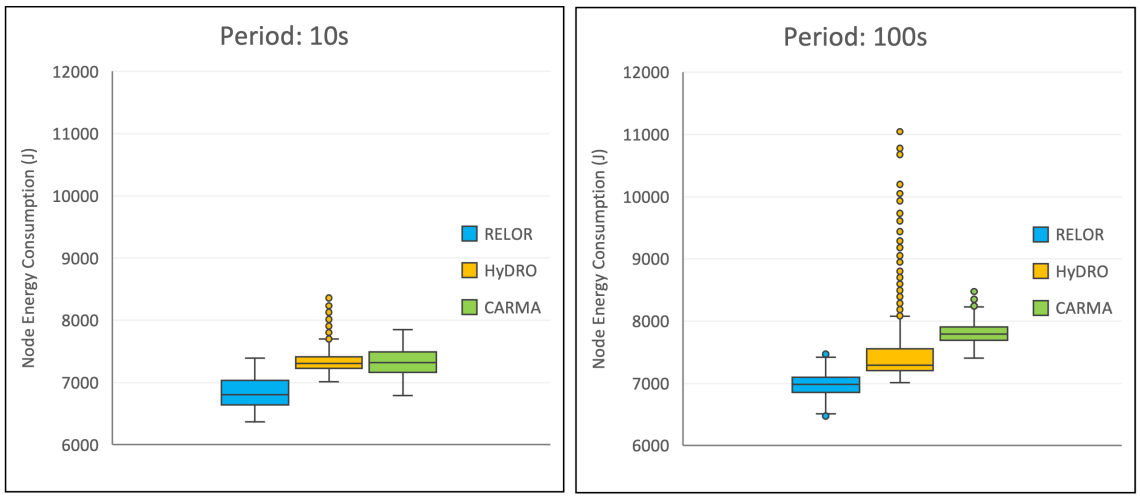

FIGURE 5.8: Average Node Energy Consumption. Scenario of 40 Nodes.

Moreover, the performance of the proposed protocol is also evaluated with one sink node (located at the center of the network) instead of three. Fig. 5.9 shows the packet delivery ratio for packet inter-generation time of 10 s, 30 s, 60 s and 100 s in the network with one sink node. The first trend is that the RELOR protocol also outperformed the other two protocols as a result of the RL-based candidate nodes set selection. Overall, all three protocols deliver packets at higher rates when a network has three sinks as compared to a network with one sink. In the case of a network with three sink nodes, packets can be received by either one of the sinks rather than simply by a single sink, as having three sinks makes the network faster

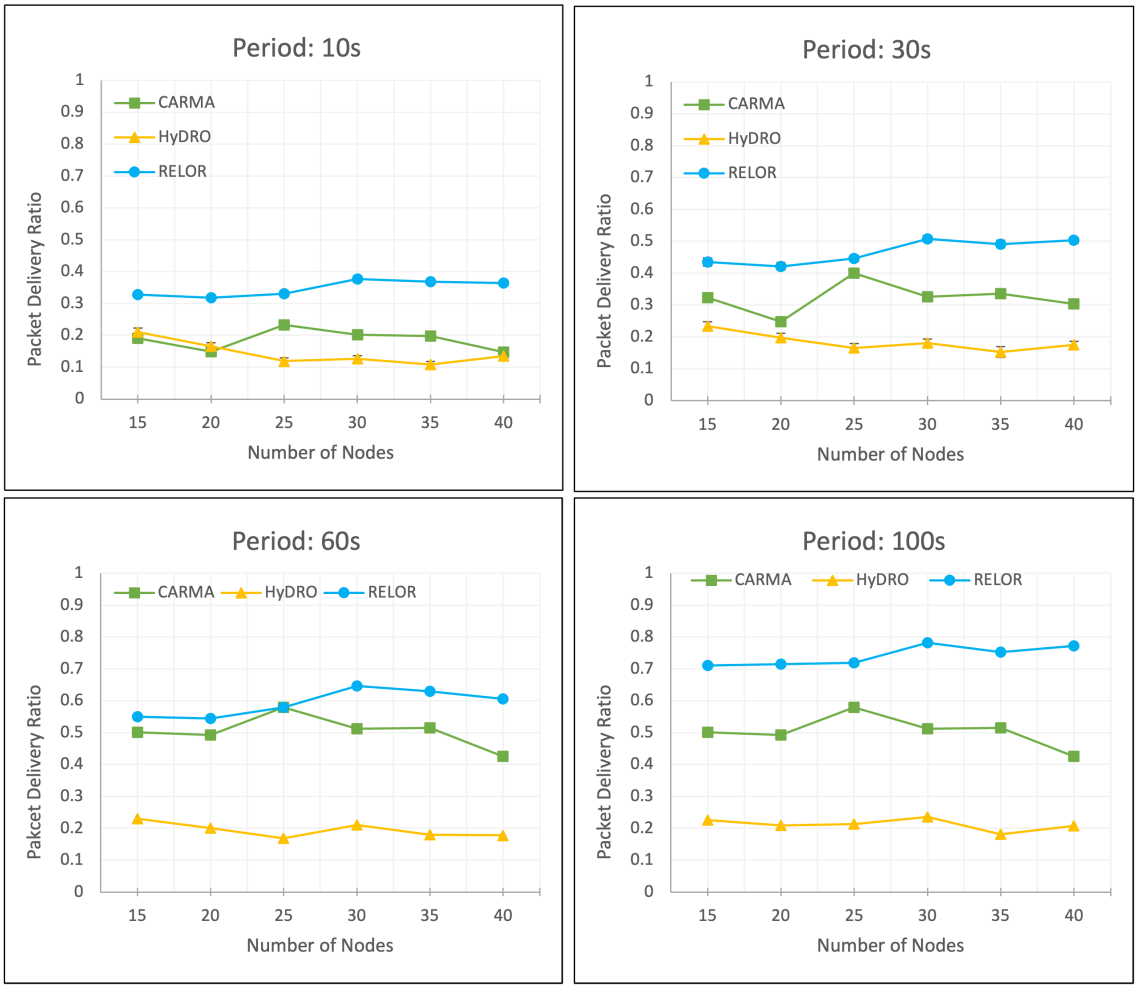

FIGURE 5.9: Packet Delivery Ratio. Scenario of 1 Sink Node

and more reliable.

Fig. 5.10 illustrates the average end-to-end delay when only one sink is defined in the network. Similar to Fig. 5.3, the end-to-end delay for the RELOR protocol is higher than those two other protocols because of the same reasons. There is a slight increase in end-to-end delay when there is only one sink node in the network, since that sink is responsible for receiving all packets in the network, resulting in increased packet collisions and packet losses as well as an increase in the number of retransmissions.

Figs. 5.11 and 5.12 show the network's overall energy consumption for scenarios involving one sink node on the surface and 15 or 40 underwater sensor nodes, respectively. In addition a comparison of nodes' energy consumption in low and high density networks with one sink node for three protocols is presented in Figs. 5.13

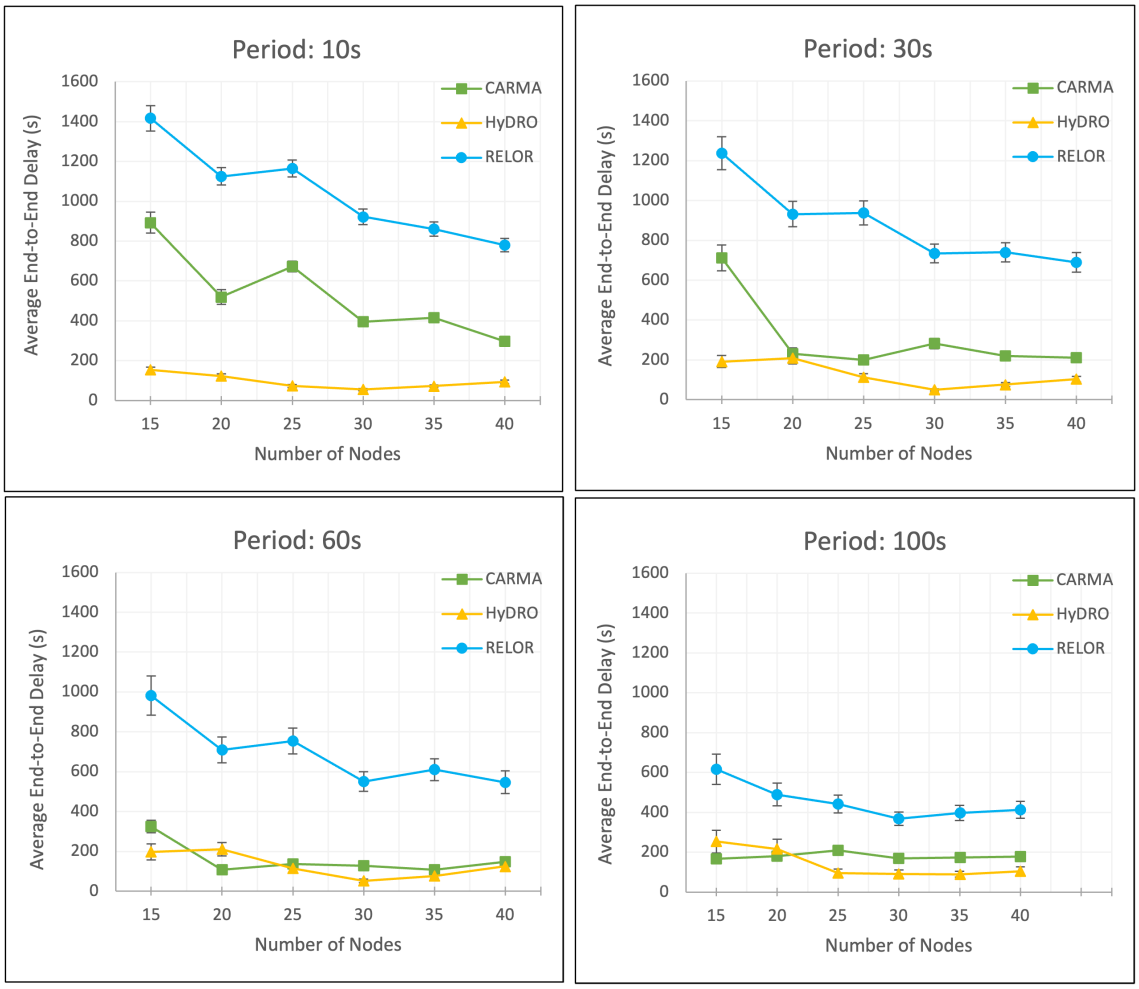

FIGURE 5.10: Average End-to-End Delay (s). Scenario of 1 Sink Node

and 5.14. The overall trend in these scenarios follow the same pattern as the scenarios with three sinks(Figs. 5.5, 5.6, 5.7 and 5.8), resulting in a lower rate of energy consumption for the RELOR protocol. Additionally, networks with a single sink node consume more energy than those with three sinks. This is due to the fact that in a network with three sinks, there is a lower rate of transmission failures and retransmissions. Nodes in a network require more energy to operate when packets are retransmitted, as this increases their energy consumption.

5.3 Conclusion

The performance of the proposed protocol is evaluated by the DESERT underwater simulator under realistic UWSN deployments and environmental conditions.

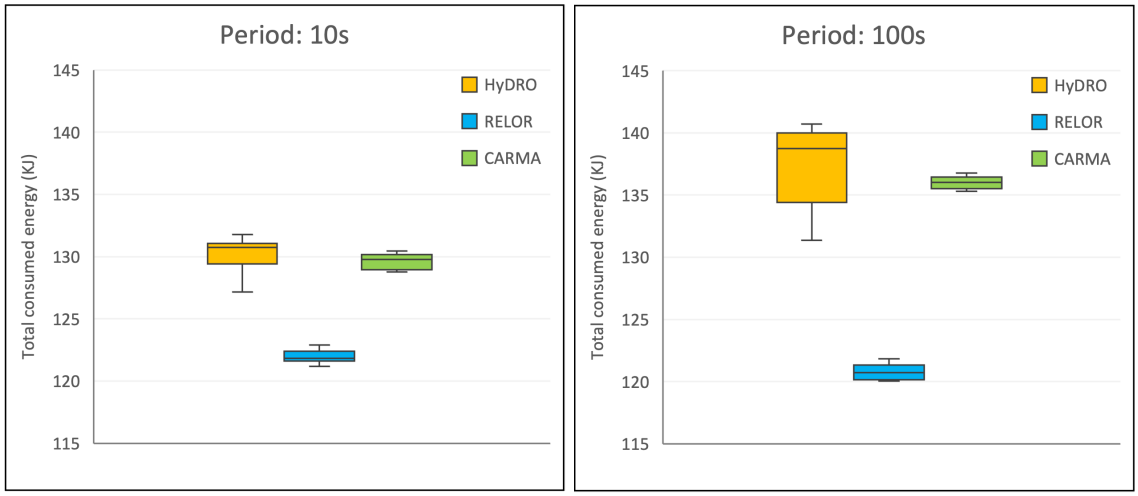

FIGURE 5.11: Total Network Energy Consumption. Scenario of 1 Sink Node and 15 Sensor Nodes

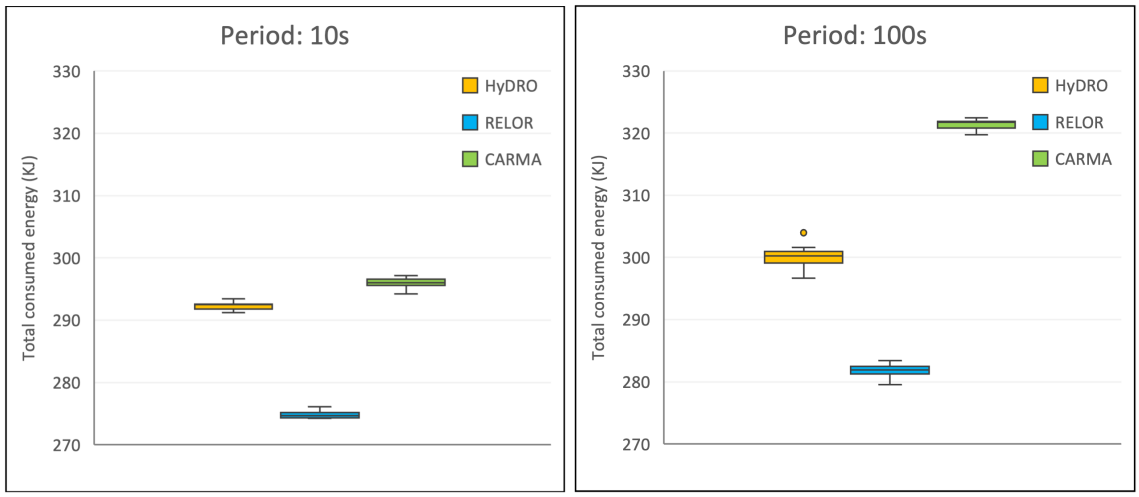

FIGURE 5.12: Total Network Energy Consumption. Scenario of 1 Sink Node and 40 Sensor Nodes

A comparison was made between the proposed protocol and two state-of-the-art protocols, CARMA and HyDRO, based on six parameters: packet delivery ratio, average end-to-end delay, number of duplicated packets received, total energy consumption and nodes' energy consumption. The proposed work outperforms two other protocols in the majority of scenarios except for end-to-end delay, which is a trade-off for higher packet delivery rates. RELOR's improved performance can be attributed to the use of Q-learning methods to choose a set of candidate nodes based on their residual energy and foreseeable harvestable energy.

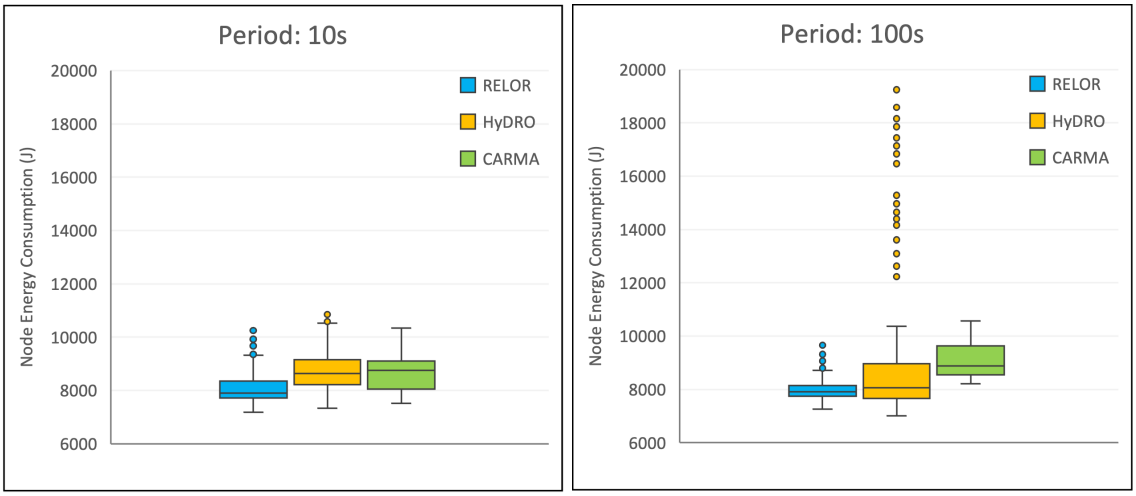

FIGURE 5.13: Average Node Energy Consumption. Scenario of 1 Sink Node and 15 Sensor Nodes

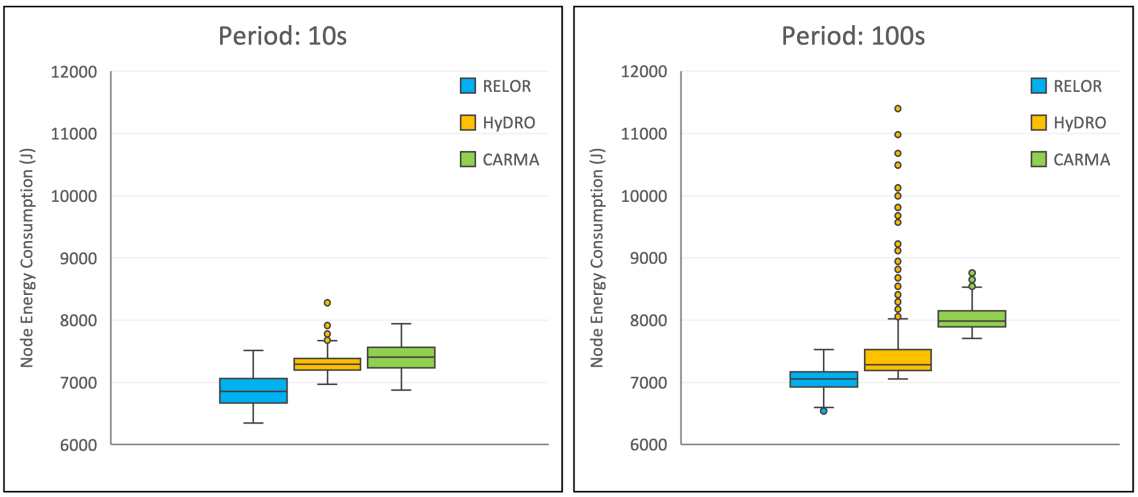

FIGURE 5.14: Average Node Energy Consumption. Scenario of 1 Sink Node and 40 Sensor Nodes

Chapter 6

Conclusion and Future Work

6.1 Conclusion

In this thesis, we investigate the design of an opportunistic routing protocol (OR) which exploits the capability of harvesting energy in the sensor nodes in underwater wireless sensor networks. We proposed the RELOR protocol, a novel reinforcement learning-based energy harvesting-aware Opportunistic Routing protocol. More specifically RELOR considers the foreseeable energy to be harvested in the neighboring nodes, the energy cost, and link quality to select the set of next-hop candidate nodes at each hop. The main goal was to select energy-efficient opportunistic routing paths from source nodes to the surface sonobuoy aimed at improving data delivery reliability while prolonging the network lifetime. To evaluate the performance of the proposed routing protocol under realistic UWSN deployments and environmental conditions, the DESERT underwater simulator was used. Simulation-based performance evaluation showed that the proposed protocol outperformed the previous state-of-the-art routing protocol for underwater networks with energy harvesting capabilities. The proposed RELOR protocol achieved an increased packet delivery ratio as compared to related work, due to the OR mechanism implemented to reduce the effects of the poor quality of individual acoustic links. Moreover, the proposed protocol achieved better results in terms of delay for scenarios of high traffic loads, and reduced energy consumption at the nodes.

6.2 Future Works

In addition to the methods used in this thesis, additional studies can be carried out. As future work, following aspect can be investigated.

As a means of supplying energy to the sensor nodes, wireless power transfer can be considered. It is possible to harvest energy from other sources, such as solar panels on the ocean surface or utilizing kinetic propeller harvesters, and then transfer it to the sensor nodes using Wireless Power Transfer (WPT). It may also be beneficial to consider ways of providing energy to mobile UWSNs and AUVs. The routing protocol can be extended to incorporate different methods of energy harvesting which can then be evaluated.

To improve the efficiency of the routing protocol and reduce the end-to-end delay in the network, the delay of the system may be considered in the reward function of the Q-learning process. Furthermore, AUVs can also be considered as part of our network, and mechanisms can be designed to accommodate their mobility.

Aside from this, we are also able to explore the possibilities of power control as a means to improve the energy efficiency of underwater sensor networks that are capable of harvesting energy.

Bibliography

[1] R. W. Coutinho, A. Boukerche, L. F. Vieira, and A. A. Loureiro, "Design guidelines for opportunistic routing in underwater networks," *IEEE Communications Magazine*, vol. 54, no. 2, pp. 40–48, 2016.

[2] I. F. Akyildiz and I. H. Kasimoglu, "Wireless sensor and actor networks: Research challenges," *Ad hoc networks*, vol. 2, no. 4, pp. 351–367, 2004.

[3] J. Heidemann, M. Stojanovic, and M. Zorzi, "Underwater sensor networks: Applications, advances and challenges," *Philosophical Transactions of the Royal Society A: Mathematical, Physical and Engineering Sciences*, vol. 370, no. 1958, pp. 158–175, 2012.

[4] H. Kaushal and G. Kaddoum, "Underwater optical wireless communication," *IEEE Access*, vol. 4, pp. 1518–1547, Apr. 2016. DOI: 10.1109/ACCESS.2016.2552538.

[5] A. Palmeiro, M. Martin, I. Crowther, and M. Rhodes, "Underwater radio frequency communications," Jul. 2011, pp. 1 –8. DOI: 10.1109/Oceans-Spain.2011.6003580.

[6] C. Gabriel, M.-A. Khalighi, S. Bourennane, P. Leon, and V. Rigaud, "Channel modeling for underwater optical communication," in *2011 IEEE GLOBECOM Workshops (GC Wkshps)*, 2011, pp. 833–837. DOI: 10.1109/GLOCOMW.2011.6162571.

[7] R. T. Rodoshi, Y. Song, and W. Choi, "Reinforcement learning-based routing protocol for underwater wireless sensor networks: A comparative survey,"

IEEE Access, vol. 9, pp. 154 578–154 599, 2021. DOI: 10.1109/ACCESS.2021.3128516.

[8] I. F. Akyildiz, D. Pompili, and T. Melodia, "Underwater acoustic sensor networks: Research challenges," *Ad hoc networks*, vol. 3, no. 3, pp. 257–279, 2005.

[9] E. Sozer, M. Stojanovic, and J. Proakis, "Underwater acoustic networks," *IEEE Journal of Oceanic Engineering*, vol. 25, no. 1, pp. 72–83, 2000. DOI: 10.1109/48.820738.

[10] M. Stojanovic and J. Preisig, "Underwater acoustic communication channels: Propagation models and statistical characterization," *IEEE communications magazine*, vol. 47, no. 1, pp. 84–89, 2009.

[11] M. Chitre, S. Shahabudeen, and M. Stojanovic, "Underwater acoustic communications and networking: Recent advances and future challenges," *Marine Technology Society Journal*, vol. 42, pp. 103–116, Mar. 2008. DOI: 10.4031/002533208786861263.

[12] R. W. Coutinho, A. Boukerche, L. F. Vieira, and A. A. Loureiro, "Geographic and opportunistic routing for underwater sensor networks," *IEEE Transactions on Computers*, vol. 65, no. 2, pp. 548–561, 2015.

[13] S El-Rabaie, D Nabil, R Mahmoud, and M. A. Alsharqawy, "Underwater wireless sensor networks (uwsn), architecture, routing protocols, simulation and modeling tools, localization, security issues and some novel trends," *Netw. Commun. Eng*, vol. 7, no. 8, pp. 335–354, 2015.

[14] H. Yan, Z. J. Shi, and J.-H. Cui, "Dbr: Depth-based routing for underwater sensor networks," in *International conference on research in networking*, Springer, 2008, pp. 72–86.

[15] J. M. Jornet, M. Stojanovic, and M. Zorzi, "Focused beam routing protocol for underwater acoustic networks," in *Proceedings of the third ACM international workshop on Underwater Networks*, 2008, pp. 75–82.

[16] R. W. L. Coutinho, A. Boukerche, L. F. M. Vieira, and A. A. F. Loureiro, "Gedar: Geographic and opportunistic routing protocol with depth adjustment for mobile underwater sensor networks," in *2014 IEEE International Conference on Communications (ICC)*, 2014, pp. 251–256. DOI: 10.1109/ICC.2014.6883327.

[17] Y. Noh, U. Lee, P. Wang, B. S. C. Choi, and M. Gerla, "Vapr: Void-aware pressure routing for underwater sensor networks," *IEEE Transactions on Mobile Computing*, vol. 12, no. 5, pp. 895–908, 2012.

[18] P. Xie, J.-H. Cui, and L. Lao, "Vbf: Vector-based forwarding protocol for underwater sensor networks," in *International conference on research in networking*, Springer, 2006, pp. 1216–1221.

[19] T. Hu and Y. Fei, "Qelar: A machine-learning-based adaptive routing protocol for energy-efficient and lifetime-extended underwater sensor networks," *IEEE Transactions on Mobile Computing*, vol. 9, no. 6, pp. 796–809, 2010. DOI: 10.1109/TMC.2010.28.

[20] R. W. Coutinho, A. Boukerche, and A. A. Loureiro, "A novel opportunistic power controlled routing protocol for internet of underwater things," *Computer Communications*, vol. 150, pp. 72–82, 2020.

[21] R. W. Coutinho and A. Boukerche, "Omus: Efficient opportunistic routing in multi-modal underwater sensor networks," *IEEE Transactions on Wireless Communications*, vol. 20, no. 9, pp. 5642–5655, 2021.

[22] A. Darehshoorzadeh and A. Boukerche, "Underwater sensor networks: A new challenge for opportunistic routing protocols," *IEEE Communications Magazine*, vol. 53, no. 11, pp. 98–107, 2015.

[23] C.-C. Kao, Y.-S. Lin, G.-D. Wu, and C.-J. Huang, "A comprehensive study on the internet of underwater things: Applications, challenges, and channel models," *Sensors*, vol. 17, no. 7, p. 1477, 2017.

[24] K. Menon, D. Pullarkatt, and M. Vinodini Ramesh, "Wireless sensor network for river water quality monitoring in india," Jul. 2012, pp. 1–7. DOI: 10.1109/ICCCNT.2012.6512437.

[25] A. Khan and L. Jenkins, "Undersea wireless sensor network for ocean pollution prevention," in *2008 3rd International Conference on Communication Systems Software and Middleware and Workshops (COMSWARE '08)*, 2008, pp. 2–8. DOI: 10.1109/COMSWA.2008.4554369.

[26] E. F. Obodoeze, L. Nwobodo, and S. Nwokoro, "Underwater real-time oil pipeline monitoring using underwater wireless sensor networks (uwsns): Case study of niger delta region," *Journal of Multidisciplinary Engineering Science and Technology (JMEST) Berlin Germany*, vol. Vol.2, pp.3597–3602, Dec. 2015.

[27] M. Kong, Y. Guo, M. Sait, *et al.*, "Underwater optical wireless sensor network for real-time underwater environmental monitoring," in *Next-Generation Optical Communication: Components, Sub-Systems, and Systems XI*, SPIE, vol. 12028, 2022, pp. 82–86.

[28] R. W. Coutinho and A. Boukerche, "North atlantic right whales preservation: A new challenge for internet of underwater things and smart ocean-based systems," *IEEE Instrumentation & Measurement Magazine*, vol. 24, no. 3, pp. 61–67, 2021.

[29] S. Srinivas, P. Ranjitha, R. Ramya, and G. K. Narendra, "Investigation of oceanic environment using large-scale uwsn and uanets," in *2012 8th International Conference on Wireless Communications, Networking and Mobile Computing*, 2012, pp. 1–5. DOI: 10.1109/WiCOM.2012.6478552.

[30] R. Marín-Pérez, J. García-Pintado, and A. F. Gómez-Skarmeta, "A real-time measurement system for long-life flood monitoring and warning applications," *Sensors (Basel, Switzerland)*, vol. 12, pp. 4213 –4236, 2012.

[31] P. Kumar, P. Kumar, P. Priyadarshini, and Srija, "Underwater acoustic sensor network for early warning generation," *2012 Oceans*, pp. 1–6, 2012.

[32] K. Casey, A. Lim, and G. Dozier, "A sensor network architecture for tsunami detection and response," *Int. J. Distrib. Sen. Netw.*, 28–43, 2008.

[33] D. P. Williams, "On optimal auv track-spacing for underwater mine detection," in *2010 IEEE International Conference on Robotics and Automation*, IEEE, 2010, pp. 4755–4762.

[34] S. Zhou and P. Willett, "Submarine location estimation via a network of detection-only sensors," *IEEE Transactions on Signal Processing*, vol. 55, no. 6, pp. 3104–3115, 2007. DOI: 10.1109/TSP.2007.893970.

[35] E. Cayirci, H. Tezcan, Y. Dogan, and V. Coskun, "Wireless sensor networks for underwater survelliance systems," *Ad hoc networks*, vol. 4, no. 4, pp. 431–446, 2006.

[36] T. Le Sage, A. Bindel, P. Conway, S. Slawson, and A. West, "Development of a wireless sensor network for embedded monitoring of human motion in a harsh environment," in *2011 IEEE 3rd International Conference on Communication Software and Networks*, IEEE, 2011, pp. 112–115.

[37] Y. Guo and Y. Liu, "Localization for anchor-free underwater sensor networks," *Computers Electrical Engineering*, vol. 39, pp. 1812–1821, Aug. 2013. DOI: 10.1016/j.compeleceng.2013.02.001.

[38] K. M. Awan, P. A. Shah, K. Iqbal, S. Gillani, W. Ahmad, and Y. Nam, "Underwater wireless sensor networks: A review of recent issues and challenges," *Wireless Communications and Mobile Computing*, vol. 2019, 2019.

[39] G. Yang, L. Dai, and Z. Wei, "Challenges, threats, security issues and new trends of underwater wireless sensor networks," *Sensors*, vol. 18, no. 11, p. 3907, 2018.

[40] M. Stojanovic, "On the relationship between capacity and distance in an underwater acoustic communication channel," *ACM SIGMOBILE Mobile Computing and Communications Review*, vol. 11, no. 4, pp. 34–43, 2007.

[41] acoustic communications group, *Micromodem overview*, https://acomms.whoi.edu/micro-modem/.

[42] R. W. Coutinho, A. Boukerche, L. F. Vieira, and A. A. Loureiro, "Underwater wireless sensor networks: A new challenge for topology control-based systems," *ACM Computing Surveys (CSUR)*, vol. 51, no. 1, pp. 1–36, 2018.

[43] S. Basagni, V. Di Valerio, P. Gjanci, and C. Petrioli, "Harnessing hydro: Harvesting-aware data routing for underwater wireless sensor networks," in *Proceedings of the Eighteenth ACM International Symposium on Mobile Ad Hoc Networking and Computing*, 2018, pp. 271–279.

[44] V. Di Valerio, F. Lo Presti, C. Petrioli, L. Picari, D. Spaccini, and S. Basagni, "Carma: Channel-aware reinforcement learning-based multi-path adaptive routing for underwater wireless sensor networks," *IEEE Journal on Selected Areas in Communications*, vol. 37, no. 11, pp. 2634–2647, 2019. DOI: 10.1109/JSAC.2019.2933968.

[45] R. Masiero, S. Azad, F. Favaro, *et al.*, "Desert underwater: An ns-miracle-based framework to design, simulate, emulate and realize test-beds for underwater network protocols," in *2012 Oceans-Yeosu*, IEEE, 2012, pp. 1–10.

[46] F. Campagnaro, R. Francescon, F. Guerra, *et al.*, "The desert underwater framework v2: Improved capabilities and extension tools," in *2016 IEEE Third Underwater Communications and Networking Conference (UComms)*, IEEE, 2016, pp. 1–5.

[47] S. Deldouzi and R. W. L. Coutinho, "A novel harvesting-aware rl-based opportunistic routing protocol for underwater sensor networks," in *Proceedings of the 24th International ACM Conference on Modeling, Analysis and Simulation of Wireless and Mobile Systems*, ser. MSWiM '21, New York, NY, USA: Association for Computing Machinery, 2021, 87–94, ISBN: 9781450390774. DOI: 10.1145/3479239.3485694. [Online]. Available: https://doi.org/10.1145/3479239.3485694.

[48] Y. Li and R. Shi, "An intelligent solar energy-harvesting system for wireless sensor networks," *EURASIP Journal on Wireless Communications and Networking*, vol. 2015, no. 1, pp. 1–12, 2015.

[49] R. Ibrahim, T. D. Chung, S. M. Hassan, K. Bingi, and S. K. binti Salahuddin, "Solar energy harvester for industrial wireless sensor nodes," *Procedia Computer Science*, vol. 105, pp. 111–118, 2017.

[50] P. Corke, P. Valencia, P. Sikka, T. Wark, and L. Overs, "Long-duration solar-powered wireless sensor networks," in *Proceedings of the 4th workshop on Embedded networked sensors*, 2007, pp. 33–37.

[51] A. Bakkali, J. Pelegri-Sebastia, T. Sogorb, A. Bou-Escriva, and A. Lyhyaoui, "Design and simulation of dual-band rf energy harvesting antenna for wsns," *Energy Procedia*, vol. 139, pp. 55–60, 2017.

[52] K Xie, Y.-M. Liu, H.-L. Zhang, and L.-Z. Fu, "Harvest the ambient am broadcast radio energy for wireless sensors," *Journal of Electromagnetic Waves and Applications*, vol. 25, no. 14-15, pp. 2054–2065, 2011.

[53] J. Zhang, Z. Fang, C. Shu, J. Zhang, Q. Zhang, and C. Li, "A rotational piezoelectric energy harvester for efficient wind energy harvesting," *Sensors and Actuators A: Physical*, vol. 262, pp. 123–129, 2017.

[54] E. Kamenar, S. Zelenika, D. Blažević, *et al.*, "Harvesting of river flow energy for wireless sensor network technology," *Microsystem Technologies*, vol. 22, no. 7, pp. 1557–1574, 2016.

[55] S. Chiacchiari, F. Romeo, D. M. McFarland, L. A. Bergman, and A. F. Vakakis, "Vibration energy harvesting from impulsive excitations via a bistable nonlinear attachment," *International Journal of Non-Linear Mechanics*, vol. 94, pp. 84–97, 2017.

[56] Y. Wu and W. Liu, "Routing protocol based on genetic algorithm for energy harvesting-wireless sensor networks," *IET Wireless Sensor Systems*, vol. 3, no. 2, pp. 112–118, 2013.

[57] M. Xiao, X. Zhang, and Y. Dong, "An effective routing protocol for energy harvesting wireless sensor networks," in *2013 IEEE wireless communications and networking conference (WCNC)*, IEEE, 2013, pp. 2080–2084.

[58] T. D. Nguyen, J. Y. Khan, and D. T. Ngo, "An effective energy-harvesting-aware routing algorithm for wsn-based iot applications," in *2017 IEEE International Conference on Communications (ICC)*, IEEE, 2017, pp. 1–6.

[59] M. K. Jakobsen, J. Madsen, and M. R. Hansen, "Dehar: A distributed energy harvesting aware routing algorithm for ad-hoc multi-hop wireless sensor networks," in *2010 IEEE International Symposium on" A World of Wireless, Mobile and Multimedia Networks"(WoWMoM)*, IEEE, 2010, pp. 1–9.

[60] D Diab, F Lefebvre, G Nassar, *et al.*, "An autonomous low-power management system for energy harvesting from a miniaturized spherical piezoelectric transducer," *Review of Scientific Instruments*, vol. 90, no. 7, p. 075 004, 2019.

[61] S. Kim, J. Y. Cho, D. H. Jeon, *et al.*, "Propeller-based underwater piezoelectric energy harvesting system for an autonomous iot sensor system," *Journal of the Korean Physical Society*, vol. 76, no. 3, pp. 251–256, 2020.

[62] D. M. Toma, J. del Rio, M. Carbonell-Ventura, and J. M. Masalles, "Underwater energy harvesting system based on plucked-driven piezoelectrics," in *OCEANS 2015-Genova*, IEEE, 2015, pp. 1–5.

[63] Y. Cha, H. Kim, and M. Porfiri, "Energy harvesting from underwater base excitation of a piezoelectric composite beam," *Smart materials and Structures*, vol. 22, no. 11, p. 115 026, 2013.

[64] F. U. Qureshi, A. Muhtaroğlu, and K. Tuncay, "Near-optimal design of scalable energy harvester for underwater pipeline monitoring applications with consideration of impact to pipeline performance," *IEEE Sensors Journal*, vol. 17, no. 7, pp. 1981–1991, 2017.

[65] X. Wang, S. Niu, Y. Yin, F. Yi, Z. You, and Z. L. Wang, "Triboelectric nanogenerator based on fully enclosed rolling spherical structure for harvesting low-frequency water wave energy," *Advanced Energy Materials*, vol. 5, no. 24, pp. 1 501 467–1 501 467, 2015.

[66] Y. Zhang, Y. Li, R. Cheng, *et al.*, "Underwater monitoring networks based on cable-structured triboelectric nanogenerators," *Research*, vol. 2022, 2022.

[67] C. Donovan, A. Dewan, H. Peng, D. Heo, and H. Beyenal, "Power management system for a 2.5 w remote sensor powered by a sediment microbial fuel cell," *Journal of Power Sources*, vol. 196, no. 3, pp. 1171–1177, 2011.

[68] G. Huang, R. Umaz, U. Karra, B. Li, and L. Wang, "A biomass-based marine sediment energy harvesting system," in *International Symposium on Low Power Electronics and Design (ISLPED)*, IEEE, 2013, pp. 359–364.

[69] R. Umaz, "Efficient power management circuit for biomass-based energy harvesting system," *International Journal of Circuit Theory and Applications*, vol. 48, no. 6, pp. 874–886, 2020.

[70] S. Carreon-Bautista, C. Erbay, A. Han, and E. Sanchez-Sinencio, "An inductorless dc–dc converter for an energy aware power management unit aimed at microbial fuel cell arrays," *IEEE Journal of Emerging and Selected Topics in Power Electronics*, vol. 3, no. 4, pp. 1109–1121, 2015.

[71] D. Zhang, F. Yang, T. Shimotori, K.-C. Wang, and Y. Huang, "Performance evaluation of power management systems in microbial fuel cell-based energy harvesting applications for driving small electronic devices," *Journal of Power Sources*, vol. 217, pp. 65–71, 2012.

[72] A. Meehan, H. Gao, and Z. Lewandowski, "Energy harvesting with microbial fuel cell and power management system," *IEEE Transactions on power electronics*, vol. 26, no. 1, pp. 176–181, 2010.

[73] A. Zayan and T. E. Vandervelde, "Intlp compounds for underwater solar energy harvesting," *MRS Advances*, vol. 3, no. 3, pp. 153–158, 2018.

[74] M. K. Amruta and M. T. Satish, "Solar powered water quality monitoring system using wireless sensor network," in *2013 International Mutli-Conference on Automation, Computing, Communication, Control and Compressed Sensing (iMac4s)*, IEEE, 2013, pp. 281–285.

[75] S. Kamal, G. M. Al-sayyad, R. Abdelmoteleb, M. Abdellatif, and S. O. Abdellatif, "Submerged solar energy harvesters performance for underwater applications," in *2019 International Conference on Innovative Trends in Computer Engineering (ITCE)*, IEEE, 2019, pp. 444–449.

[76] P. P. Jenkins, S. Messenger, K. M. Trautz, *et al.*, "High-bandgap solar cells for underwater photovoltaic applications," *IEEE Journal of Photovoltaics*, vol. 4, no. 1, pp. 202–207, 2013.

[77] M. Abdellatif, S. Maher, G. Al-sayyad, and S. Abdellatif, "Implementation of a low cost, solar charged rf modem for underwater wireless sensor networks," *International Journal on Smart Sensing and Intelligent Systems*, vol. 13, pp. 1–11, Jan. 2020. DOI: 10.21307/ijssis-2020-015.

[78] J.-K. Kim, E. Lee, H. Kim, C. Johnson, J. Cho, and Y. Kim, "Rechargeable seawater battery and its electrochemical mechanism," *ChemElectroChem*, vol. 2, no. 3, 2014.

[79] M. Shinohara, E. Araki, M. Mochizuki, T. Kanazawa, and K. Suyehiro, "Practical application of a sea-water battery in deep-sea basin and its performance," *Journal of Power Sources*, vol. 187, no. 1, pp. 253–260, 2009.

[80] H. F. Rezaei, A. Kruger, and C. Just, "An energy harvesting scheme for underwater sensor applications," in *2012 IEEE International Conference on Electro/Information Technology*, IEEE, 2012, pp. 1–4.

[81] G. N. Sivakami, V. Perarasu, and S. S. Murugan, "Study on suitable electrode for energy harvesting using galvanic cell in seawater," in *Proceedings of the Fourth International Conference in Ocean Engineering (ICOE2018)*, Springer, 2019, pp. 629–638.

[82] U. Gule, *Implantable and wearable sensors for assistive technologies*, Available at https://www.sciencedirect.com/topics/engineering/piezoelectric-effect.

[83] F.-R. Fan, Z.-Q. Tian, and Z. Lin Wang, "Flexible triboelectric generator," vol. 1, no. 2, pp. 328–334, 2012.

[84] R. Guida, E. Demirors, N. Dave, and T. Melodia, "Underwater ultrasonic wireless power transfer: A battery-less platform for the internet of underwater things," *IEEE Transactions on Mobile Computing*, 2020.

[85] Y. Noh, U. Lee, S. Lee, *et al.*, "Hydrocast: Pressure routing for underwater sensor networks," *IEEE Transactions on Vehicular Technology*, vol. 65, no. 1, pp. 333–347, 2015.

[86] R. W. Coutinho, A. Boukerche, L. F. Vieira, and A. A. Loureiro, "Enor: Energy balancing routing protocol for underwater sensor networks," in *2017 IEEE International Conference on Communications (ICC)*, IEEE, 2017, pp. 1–6.

[87] S. Basagni, V. Di Valerio, P. Gjanci, and C. Petrioli, "Marlin-q: Multi-modal communications for reliable and low-latency underwater data delivery," *Ad Hoc Networks*, vol. 82, pp. 134–145, 2019.

[88] E. P. C. Júnior, L. F. Vieira, and M. A. Vieira, "Captain: A data collection algorithm for underwater optical-acoustic sensor networks," *Computer Networks*, vol. 171, p. 107 145, 2020.

[89] M. Han, J. Duan, S. Khairy, and L. X. Cai, "Enabling sustainable underwater iot networks with energy harvesting: A decentralized reinforcement learning approach," *IEEE Internet of Things Journal*, vol. 7, no. 10, pp. 9953–9964, 2020.

[90] R. Wang, A. Yadav, E. A. Makled, O. A. Dobre, R. Zhao, and P. K. Varshney, "Optimal power allocation for full-duplex underwater relay networks with energy harvesting: A reinforcement learning approach," *IEEE wireless communications letters*, vol. 9, no. 2, pp. 223–227, 2019.

[91] T. MARINE, *Benthos directional acoustic transponder (dat)*, http://www.teledynemarine.com/Lists/Downloads/Benthos_DAT_Datasheet.pdf, Accessed: 2021-07-01, 2021.

[92] EvoLogics, *Evologics s2cr 18/34 product information*, https://evologics.de/web/content/16559?unique=277076761b6fad35da5fb71bbf008bd08624fba9, Accessed: 2021-07-01, 2021.